Journal of Hazardous Materials 476 (2024) 135099

Contents lists available at ScienceDirect

Journal of Hazardous Materials

journal homepage: www.elsevier.com/locate/jhazmat

Transformation of antibiotics to non-toxic and non-bactericidal products by laccases ensure the safety of *Stropharia rugosoannulata*

Shuxue Zhao [a,b], Xiaohang Li [a,b], Xingdong Yao [a], Wei Wan [a], Lili Xu [a], Lizhong Guo [a], Jie Bai [b], Chunhui Hu [c,*], Hao Yu [a,*]

[a] Shandong Provincial Key Laboratory of Applied Mycology, School of Life Sciences, Qingdao Agricultural University, Qingdao 266109, Shandong Province, China
[b] College of Environmental Science and Engineering, Ocean University of China, Qingdao 266100, Shandong Province, China
[c] Instrumental analysis center of Qingdao Agricultural University, Qingdao 266109, Shandong Province, China

HIGHLIGHTS

- First comprehensive study on the potential impacts of antibiotics on the production of *S. rugosoannulata*.
- Elucidation of the molecular mechanisms by which *S. rugosoannulata* counteracts the effects of antibiotics.
- Biodegradation by secreted proteins was the main antibiotic removal mechanism of *S. rugosuannulata*.
- Two laccases, SrLAC1 and SrLAC9, responsible for antibiotics degradation were characterized.
- None of the *S. rugosoannulata* fruiting bodies from seven provinces in China contains detectable antibiotic-resistance genes.

GRAPHICAL ABSTRACT

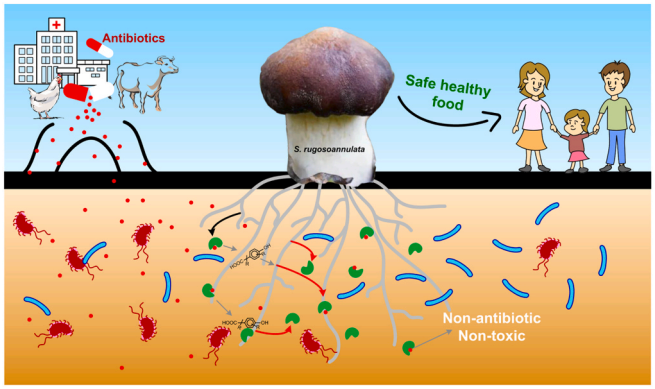

ARTICLE INFO

Keywords:
Stropharia rugosoannulata
Laccase
Antibiotics
Biodegradation

ABSTRACT

The substantial use of antibiotics contributes to the spread and evolution of antibiotic resistance, posing potential risks to food production systems, including mushroom production. In this study, the potential risk of antibiotics to *Stropharia rugosoannulata*, the third most productive straw-rotting mushroom in China, was assessed, and the underlying mechanisms were investigated. Tetracycline exposure at environmentally relevant concentrations

Abbreviation: 2,6-DMP, 2,6-dimethoxyphenol; 3D, three dimensional; AA, auxiliary activities; ABTS, 2,2′-azino-bis (3-ethylbenzothiazoline-6-sulfonate); ARB, antibiotic resistant bacteria; ARGs, antibiotic resistance genes; CAT, catalase; CAZymes, carbohydrate active enzymes; CE, carbohydrate esterase; CTC, chlortetracycline; DCE, doxycycline; DCL, doxycycline hydrochloride; EFN, enrofloxacin; GH, glycoside hydrolase; GT, glycosyltransferase; HBT, 1-hydroxybenzotriazole; HPLC, high performance liquid chromatography; LB medium, Luria-Bertani medium; HPLC-ESI-Q-TOF-MS, ultra-high-performance liquid chromatography-high resolution mass spectrometry; LMS, laccase-mediator systems; MDA, malondialdehyde; MFN, moxifloxacin; MYN, maltose yeast extract media; MYNT, MYN with the addition of TET; NFN, norfloxacin; OTC, oxytetracyclin; PCA, principal component analysis; PDA, potato dextrose broth agar medium; PDB, potato dextrose broth medium; PL, polysaccharide lyase; POD, peroxidase; QNs, quinolones; SAA, sulfadiazine; SAs, sulfonamides; SDS-PAGE, sodium dodecyl sulfate polyacrylamide gel electrophoresis; SMX, sulfamethoxazole; SMY, sulfamethoxypyridazine; SOD, superoxide dismutase; SyA, syringic acid; TCs, tetracyclines; TEST, toxicity estimation software tool; TET, tetracycline; YPD, yeast extract-peptone-dextrose.

* Correspondence to: 700 Changcheng Road, Chengyang District, Qingdao, Shandong Province, China.
E-mail addresses: hollyhuchunhui@163.com (C. Hu), yuhaosunshine@163.com (H. Yu).

https://doi.org/10.1016/j.jhazmat.2024.135099
Received 27 March 2024; Received in revised form 18 June 2024; Accepted 2 July 2024
Available online 3 July 2024
0304-3894/© 2024 Published by Elsevier B.V.

Food safety
Mushroom

(<500 μg/L) did not influence the growth of *S. rugosoannulata* mycelia, while high concentrations of tetracycline (>500 mg/L) slightly inhibited its growth. Biodegradation was identified as the main antibiotic removal mechanism in *S. rugosoannulata*, with a degradation rate reaching 98.31 % at 200 mg/L tetracycline. High antibiotic removal efficiency was observed with secreted proteins of *S. rugosoannulata*, showing removal efficiency in the order of tetracyclines > sulfadiazines > quinolones. Antibiotic degradation products lost the ability to inhibit the growth of *Escherichia coli*, and tetracycline degradation products could not confer a growth advantage to antibiotic-resistant strains. Two laccases, SrLAC1 and SrLAC9, responsible for antibiotic degradation were identified based on proteomic analysis. Eleven antibiotics from tetracyclines, sulfonamides, and quinolones families could be transformed by these two laccases with degradation rates of 95.54–99.95 %, 54.43–100 %, and 5.68–57.12 %, respectively. The biosafety of the antibiotic degradation products was evaluated using the Toxicity Estimation Software Tool (TEST), revealing a decreased toxicity or no toxic effect. None of the *S. rugosoannulata* fruiting bodies from seven provinces in China contained detectable antibiotic-resistance genes (ARGs). This study demonstrated that *S. rugosoannulata* can degrade antibiotics into non-toxic and non-bactericidal products that do not accelerate the spread of antibiotic resistance, ensuring the safety of *S. rugosoannulata* production.

1. Introduction

Antibiotics have been extensively used for the treatment and prevention of bacterial infections in clinical settings and the animal farming industry. Reports indicate an annual global usage of more than 100,000 tons of antibiotics [1–3]. Following consumption, only a fraction of antibiotics can be absorbed and metabolized *in vivo*, with the majority being released into the environment in their intact form [4]. Antibiotics can be regarded as "pseudo-persistent" organic contaminants in the environment owing to their continuous emission and resistance to degradation [5]. Antibiotic concentrations of up to 400 μg/kg(L) have been detected in the environments [6]. This contributes to the spread of resistance by exerting unprecedented selection pressures on the microbiome, promoting the dissemination of antibiotic resistance genes (ARGs) to numerous bacterial species. Antibiotic-resistant bacteria (ARB) pose a serious threat to global public health and food safety. The widespread presence of antibiotics in agroecosystems poses a potential threat to food safety, and many ARGs have been detected in vegetables, fruits, and cereals [4,7,8]. Consequently, evaluating the potential risks of antibiotic effects on the growth and products of these foods, including edible mushrooms, is imperative.

Edible mushrooms have long been consumed by humans for their nutritional and medicinal benefits [9,10]. The majority of mushrooms consumed by humans are now sourced from commercial cultivation rather than gathered outdoors [11]. Mushroom cultivation methods can be categorized by substrate utilization and cultivation technology. Wood-rotting mushrooms are commonly grown in sterilized substrates within cultivation bottles or bags, whereas straw-rotting mushrooms are typically cultivated using compost substrates either on the ground or on shelves covered with casting soil [12,13]. According to their cultivation method, straw-rotting mushrooms can directly interact with environmental factors such as antibiotics found in soil and surface runoff. On the one hand, the compost substrates used for cultivating straw-rotting mushrooms consist of crop straw and livestock manure, which serves as a nitrogen source for mushroom growth [14]. However, livestock manure residues in the environment often contain high concentrations of antibiotics like tetracyclines (TCs), quinolones (QNs), and sulfonamides (SAs) [15]. The use of manure-derived materials in agriculture contributes to elevated levels of antibiotic residues, ARB, and ARGs [16]. Although composting can reduce most of the ARB and ARGs in livestock manure [15,17], some residues may still remain in the compost substrates for mushroom production. Therefore, antibiotics remaining in compost could affect the growth of mushrooms during the cultivation processes. In China, many straw-rotting mushrooms are still cultivated directly on the ground by smallholder farmers, exposing them to antibiotic residues in soil and runoff, which can also impact cultivation. Researchers found that residual antibiotics are detectable in most Chinese soils [6,18]. ARB and ARGs may be distributed into the mushroom fruiting bodies, posing potential safety risks to consumers.

Removing antibiotics is crucial to mitigate their impact on mushroom production. However, physical and chemical methods are generally unsuitable for removing antibiotics during mushroom production. Most edible mushrooms belong to the category of white-rot fungi (WRF), which naturally possess the ability to degrade various organic pollutants, including antibiotics. WRF produce a range of extracellular enzymes such as laccase (EC 1.10.3.2), manganese peroxidase (EC 1.11.1.13), and lignin peroxidase (EC 1.11.1.14), which are essential for decomposing recalcitrant organic compounds like lignocellulose, polycyclic aromatic hydrocarbons, and pesticides [19]. These extracellular enzymes form the primary enzyme system through which fungi degrade antibiotics [20]. Laccase, an oxidoreductase, utilizes molecular oxygen as the terminal electron acceptor and catalyzes the oxidation of aromatic compounds, particularly phenolic compounds. It is recognized as a green catalyst with significant potential in dye decolorization [21], as well as the degradation of pesticides and antibiotics [22,23]. Suda et al. demonstrated that laccase from the white rot fungus *Trametes versicolor* could degrade tetracycline (TET), chlorotetracycline, doxycycline, and oxytetracycline in the presence of redox mediator 1-hydroxybenzotriazole (HBT) [24]. Furthermore, laccase from *T. versicolor* showed degradation capabilities for norfloxacin (NFN), enrofloxacin (EFN), and moxifloxacin (MFN), achieving degradation percentages of 93.7 %, 65.4 %, and 77.0 %, respectively [25]. The application of laccase from white-rot fungi holds promise for antibiotic removal. However, the specific mechanism by which laccase degrades antibiotics in these fungi is still unclear. *S. rugosoannulata* is a widely cultivated edible mushroom in China and northern temperate zones throughout the world, ranking as the third most productive straw-rotting mushroom in China after *Agaricus bisporus* and *Volvariella volvacea*. Predominantly cultivated on the ground by smallholder farmers [26], *S. rugosoannulata* is susceptible to the influence of antibiotics. Research indicates that *S. rugosoannulata* shows considerable potential for bioremediation, demonstrates the capability to degrade various environmental pollutants, such as synthetic dyes, polycyclic aromatic hydrocarbons, 2,4,6-trinitrotoluene [27], bisphenol A [28], and dibenzo-*p*-dioxins and dibenzofurans [29], as well as antibiotics [30]. Nevertheless, the potential impact of antibiotics on the growth of *S. rugosoannulata,* as well as the molecular mechanisms involved in antibiotic degradation, remain poorly understood.

This study systematically examined the impact of antibiotics on the growth of *S. rugosoannulata* mycelia. It investigated *S. rugosoannulata*'s ability to degrade antibiotics and elucidated the underlying mechanisms of antibiotic degradation. The Toxicity Estimation Software Tool (TEST) and *Escherichia coli* growth inhibition experiments were utilized to assess the potential toxicity of antibiotic degradation products. Additionally, the study determined the presence or absence of ARGs in the fruiting bodies of *S. rugosoannulata* collected from seven provinces in China. Based on these findings, the potential risk posed by antibiotics to the safety of *S. rugosoannulata* was thoroughly evaluated.

2. Materials and methods

2.1. Chemicals and strains

Tetracycline (TET, 99%) was purchased from Solarbio (Beijing, China). Doxycycline hydrochloride (DCL, 95–102 %), doxycycline (DCE, ≥98 %), oxytetracycline (OTC, ≥98 %), chlortetracycline (CTC, 98 %), sulfamethoxazole (SMX, 98 %), sulfadiazine (SAA, 98 %), sulfamethoxypyridazine (SMY, 98 %), norfloxacin (NFN) (98 %), moxifloxacin (MFN) (98 %), and enrofloxacin (EFN) (98 %) were purchased from Shanghai Macklin Biochemical Technology Co., Ltd (Table S1). The laccase mediator 2,2′-azino-bis (3-ethylbenzothiazoline-6-sulfonate) (ABTS, >99 %), 2,6-Dimethoxyphenol (2,6-DMP, 99 %), HBT (≥97 %) and syringic acid (SyA, 98 %) were also purchased from Shanghai Macklin Biochemical Technology Co., Ltd. All other reagents used in this study were of analytical grade unless otherwise specified. *S. rugosoannulata* GL0170 (also known as NCMCCNO230170) was provided by the Laboratory of Mushroom Precision Breeding (mushroomlab.cn). The *S. rugosoannulata* strain GL0170 used in this study was isolated from Inner Mongolia and domesticated by our lab for commercial cultivation. It has been successfully cultivated in several regions in China including Inner Mongolia, Shandong, and Gansu provinces. In our previous study, the high-quality genome of this strain was characterized [31]. *E. coli* Trans-T1 and *Pichia pastoris* GS115 competent cells were purchased from TransGen Biotech (Beijing, China). *E. coli* Trans-T1 was cultured in Luria Bertani (LB) broth, and *P. pastoris* was cultivated in yeast extract-peptone-dextrose (YPD) medium.

2.2. The impact of tetracycline on the growth of S. rugosoannulata

The mycelia of strain *S. rugosoannulata* GL0170 were cultivated on potato dextrose broth agar (PDA) medium, consisting of 200 g/L potato, 20 g/L dextrose, 20 g/L agar, 100 μM $CuSO_4$, 100 μM $MgSO_4$. The initial concentrations of TET were 0, 10, 100, 250, and 500 μg/L, respectively. The growth status of the *S. rugosoannulata* was observed after cultivating in the dark at 25 °C for 8 days. Simultaneously, *S. rugosoannulata* was cultivated in potato dextrose broth (PDB) medium with the same TET concentrations. Six biological replicates were set for each concentration. After 8 days, three replicates were centrifuged at 8000 g for 10 min, dried at 60 °C until a constant weight was achieved, and the dry weight of mycelium was measured. The other three biological parallels were used to determine the intracellular antioxidant enzyme activities (superoxide dismutase (SOD), peroxidase (POD), and catalase (CAT)) and malondialdehyde (MDA) content in *S. rugosoannulata*. Refer to the supplementary materials (Text S1) for more details. Further measurements were conducted to assess the growth status of the mycelium of *S. rugosoannulata* exposed to TET at concentrations of 0, 100, 250, 500, 1000 mg/L, respectively. The dry weight measurement method for *S. rugosoannulata* mycelium was the same as described above.

2.3. Assessment of S. rugosoannulata to remove antibiotics in liquid cultures

To verify the adsorption ability of *S. rugosoannulata* mycelium and the degradation ability of extracellular proteins to antibiotics during the growth process, *S. rugosoannulata* was inoculated at an 8 % (v/v) inoculation volume and cultivated in darkness. On the 6th day of cultivation, TET was added at concentrations of 50 and 200 mg/L, respectively. The control group was not inoculated with *S. rugosoannulata* and was incubated on a shaking bed at 25 ℃ and 125 rpm. On the 8th day, TET was extracted from the mycelium and fermentation broth using ethyl acetate, and the residual TET was determined by high-performance liquid chromatography (HPLC). The HPLC analysis was performed using a Waters Alliance equipped with a diode array detector and a C18 column (Waters Spherisorb ODS2, 4.6 mm × 250 mm, 5 μm, Massachusetts, United States). The mobile phase consisted of 30 % (v/v) acetonitrile and 70 % (v/v) ddH_2O (0.1 % trifluoroacetic acid) at a flow rate of 1.0 mL/min [32,33]. The degradation rate of antibiotics was calculated using the following formula [34]:

$$\text{Degradation rate (\%)} = (C_i - C_d)/C_i \times 100\%$$

C_i was the integrated area of antibiotics in the control group, and C_d was the integrated area of antibiotics in the culture strain.

The effect of adding different concentrations of TET (0, 100, 250, 500, 1000, and 2000 mg/L), 100 mg/L OTC, and 100 mg/L DCL on the growth of *E. coli* in *S. rugosoannulata* fermentation broth was verified. The effects of *S. rugosoannulata* fermentation broth on the growth of TET-sensitive *E. coli* cells and TET-resistant *Alcaligenes faecalis* cells, before and after the degradation of 50 mg/L TET, were measured (detailed information is available in the supplementary materials Text S4). Real-time quantitative PCR (Applied biosystems, QuantStudio 5) was used to determine the proportion of growth of the two strains. The primers for *E. coli* detection were EC01-F/R and the primers for *A. faecalis* detection were AF02-F/R (Table S2). In addition to individual antibiotics, the inhibition rate of *E. coli* after *S. rugosoannulata* degradation of mixed antibiotics was also measured, with TCs and QNs at a concentration of 1 mg/L and SAs at a concentration of 120 mg/L, respectively.

2.4. Secretome analysis

S. rugosoannulata was inoculated with 8 % (v/v) inoculation volume in two different culture media: PDB and MYN (maltose yeast extract medium: 10 g/L maltose, 0.6 g/L, yeast extract, 7 g/L KH_2PO_4, 2 g/L K_2HPO_4, 0.1 g/L $MgSO_4 \cdot 7\ H_2O$, 0.1 g/L $(NH_4)_2SO_4$). On the 6th day of cultivation, a final concentration of 100 mg/L TET was added. The fermentation broth of *S. rugosoannulata* was taken every 12 h to determine its inhibition on the growth of *E. coli*.

At the same time, *S. rugosoannulata* was cultured in MYN and PDB, with TET added after 6 days of cultivation, designated as PDBT and MYNT. The laccase activity of *S. rugosoannulata* was measured on the 6th day (before TET addition) and the 8th day (48 h after TET addition) of cultivation in different media (see supplementary materials Text S5). The culture supernatant of *S. rugosoannulata* in the PDB, PDBT, and MYN groups on day 8 was used for protein extraction using the phenol method [35]. Peptide was prepared by the Strap method [36] and the peptide concentration was measured by NanoDrop (Thermal Fisher). Peptide samples were evaporated on an RVC 2–25 CD plus vacuum concentrator (Christ, Osterode am Harz, Germany). LC-MS/MS analysis was performed using an EASY-Nano system coupled with Orbitrap Fusion™ Tribrid™ detectors (Thermo Fisher). The raw data were normalized using Proteome Discovery 3.0. The production process of secretome analysis is described in the supplementary materials. The treated data were further analyzed using Perseus software [37].

2.5. Protein expression and purification

S. rugosoannulata GL0170 was inoculated in PDB medium and cultivated in darkness at 25 °C for 7 days. The mycelia were collected and ground with liquid nitrogen. Total RNA was extracted using Trizol reagent (Takara, Japan) according to the manufacturer's instructions. Reverse transcription was performed using the Hifair III 1st Strand cDNA Synthesis Kit (gDNA digest plus) (Cat No. 11139; Yeasen Biotechnology (Shanghai) Co., Ltd.). The *SrLAC1 and SrLAC9* genes were amplified with primers listed in the supplementary material (Table S2) and inserted into the pPIC9K plasmid. The pPIC9K-*SrLAC1* and pPIC9K-*SrLAC9* plasmids were transformed into *P. pastoris* GS115 by electroporation (MicroPulser Electroporator, Bio-Rad, Munich, Germany) at 1500 V and 5 ms. The induction time (48 h, 72 h, 96 h, 120 h, 144 h), the concentration of methanol addition (0.5 %, 1 %, 1.5 %), and the bottling amount (1/10, 1/5, 2/5) were optimized. Specific procedures for

constructing and expressing recombinant strains can be found in the supplementary materials (Text S6,7,8). Proteins purification was performed according to the method reported by Yu et al. [38]. The molecular weight was evaluated by 12 % sodium dodecyl sulfate polyacrylamide gel electrophoresis (SDS-PAGE).

2.6. Lacccase activity assay and kinetic study

The pH dependency (2.0 - 7.0) of SrLAC1 and SrLAC9 was measured using purified enzyme, 0.5 mM ABTS, and 50 mM malonic acid buffer in different pH levels at 25 ℃. The effect of temperature on SrLAC1 and SrLAC9 activity was determined at 30 - 90 ℃ with the optimum pH. The thermal stability of SrLAC1 and SrLAC9 was assessed by incubating the enzyme in 50 mM malonic acid buffer for 0 - 4 h at 60 ℃ and measuring the remaining activity. The amino acid composition and content of C, H, O, N, and S elements in SrLAC1 and SrLAC9 were analyzed using online tools on the Expasy server (https://web.expasy.org/protparam/).

The K_m and V_{max} for SrLAC1 and SrLAC9 were determined in 50 mM malonic acid buffer (pH 3.0) containing 0–0.5 mM ABTS or 0–5 mM 2,6-DMP at 60 ℃ by non-linear regression analysis using the Michaelis-Menten model with GraphPad Prism 8.0 (GraphPAD Software, Inc., San Diego, CA, United States). The initial molar concentrations of SrLAC1 and SrLAC9 in the reaction mixture were 2.40 μM and 4.01 μM, respectively. The k_{cat} and catalytic efficiency (k_{cat}/K_m) of SrLAC1 (0.142 mg/mL) and SrLAC9 (0.230 mg/mL) were determined using K_m and V_{max}. The enzyme activity of SrLAC1 and SrLAC9 was also assessed by adding different metal ions (Li^+, Na^+, Mg^{2+}, K^+, Ca^{2+}, Mn^{2+}, Cu^{2+}, Zn^{2+}, Cd^{2+}, Mo^{2+}, Co^{2+}, and Fe^{2+}) at final concentration of 5 mM or 10 mM. Additionally, the effect of various inhibitors, such as EDTA, methanol, acetonitrile, acetone, and ethanol on SrLAC1 and SrLAC9 activity was assayed.

2.7. Structure prediction

The three-dimensional (3D) homology models of SrLAC1 and SrLAC9 were generated using the SwissModel online server [39] (https://swissmodel.expasy.org/). Structural analysis of SrLAC1 and SrLAC9 was conducted using InterPro (http://www.ebi.ac.uk/interpro/search/sequence/). The phylogenetic tree was constructed using MEGA X software. Motifs prediction was performed on the MEME website (https://meme-suite.org/meme/tools/meme).

2.8. Degradation of antibiotics

We compared the degradation rates of TET by SrLAC1 and SrLAC9 in the presence or absence of mediators (ABTS, HBT, SyA). The reaction mixing consisted of 50 mM malonic acid buffer (pH 3.0), 10 mM $CuSO_4$, 50 mg/L TET, 0.5 U SrLAC1 or SrLAC9, and 1 mM mediator. Reactions were conducted at 150 rpm and 30 °C for 3 h. Sterile water was used as a control in place of SrLAC1 and SrLAC9. To terminate the reaction, four volumes of methanol were added, and the supernatant was collected for HPLC analysis to determine the remaining antibiotics. Additionally, the degradation rates of TET (50 mg/L) by SrLAC1 and SrLAC9 with different mediator concentrations (0.2, 0.5, 1, 2 mM) were measured. The degradation rates by SrLAC1 and SrLAC9 with different initial TET concentrations (25–400 mg/L) in 1 mM mediators were also measured.

2.9. Identification of degradation products

The degradation products were analyzed using ultra-high-performance liquid chromatography-high resolution mass spectrometry (HPLC-ESI-Q-TOF-MS, ThermoFisher Scientific, USA). Samples were analyzed on a ZORBAX RRHD Eclipse Plus C18 column (100 × 2.1 mm.1.8 μm, Agilent, State of California, USA) with an injection volume of 1 μL. The mobile phases consist of 0.1 % formic acid (A) and methanol (B), employing a gradient elution profile (A/B, v/v): 98:2 from 0–1 min, 2:98 at 9–12 min, and 98:2 at 13–15 min. The flow rate was set at 0.35 mL/min. Tandem mass spectrometer analysis was performed with an electrosprayionization (ESI) source in positive mode with a spray voltage of 3.0 kV and acapillary temperature was 320 ℃ [32].

The mobile phases for detecting the SAA were methanol (A) and distilled water (B), using a gradient elution (A/B, v/v) starting at 90:10 from 0 to 0.5 min, changing to 40:60 from 0.5 to 2.0 min, returning to 90:10 from 2.0 to 4.0 min, and finally to 10:90 from 4.0 to 6.0 minThe flow rate was set at 0.30 mL/min, and the column temperature was set as 30 ℃. Mass spectrometry (MS/MS) was performed in negative electrospray ionization mode. Ion source and desolvation temperature were 150 ℃ and 350 ℃, respectively [40]. MS acquisition utilized full scan mode from 70 to 1000 Da at a resolution of 70,000. Mass spectra were processed using Compound Discover software 3.0 (ThermoFisher Scientific). Additionally, we assessed measured the degradation rates of SrLAC1 and SrLAC9 on TCs (excluding tetracyclines), SAs, and QNs in the presence of 1 mM mediators (ABTS, HBT, SyA).

2.10. Safety assessment

The effects of TET, DCL, and their degradation products on four aspects of Fathead minnow LC50 (96 hr), *Daphnia magna* LC50 (48 hr), Mutagenicity, and Developmental Toxicity were analyzed using the TEST method [41]. The residual antimicrobial activity of the antibiotics was assessed through the growth of *E.coli* [42]. Additionally, we examined the impact of TET and its degradation products by SrLAC1 or SrLAC9 on the growth of mixed strains of *E. coli* and *A. faecalis*, as detailed in Supplementary materials Text S9.

2.11. Detection of ARG in the fruiting body of S. rugosoannulata

We purchased commercially produced fruiting bodies of *S. rugosoannulata* from seven cultivation bases in Beijing, Shandong, Henan, Anhui, Chongqing, Sichuan, and Yunnan provinces in China. The surfaces of the fruiting body were rinsed with sterile water without disinfection, and genomic DNA was extracted using a reagent kit (see supplementary material). Fifty commonly detectable ARGs in compost were selected according to the previous study [17]. Only genes with Ct values less than 31 and correct sequences after sequencing were considered positive [43].

2.12. Statistical analysis

All determinations in this study were performed in triplicate. Data comparison was statistically analyzed using *t*-test by Origin software. A p-value of ≤ 0.05 was considered statistically significant.

3. Results and discussion

3.1. Exposure to antibiotics

Antibiotics represent one of the primary contaminants in compost, soil, and surface runoff [2]. Hence, investigating their impact on *S. rugosoannulata* is imperative. Considering that TET is one of the most commonly detected antibiotics in the soil of China [18,44], the potential influence of TET on *S. rugosoannulata* mycelia was evaluated after 8 days of exposure based on growth and oxidative-stress response. As illustrated in Fig. 1, the growth rate and dry weight of solid (Fig. 1a) and submerged (Fig. 1b) cultivated mycelia were almost identical in the low TET concentration (< 500 μg/L) exposure group and the control (without TET). We further examined the antioxidant system associated with abiotic stress in different groups of submerged cultivation. Activities of CAT and SOD enzymes did not change in TET exposure groups (Fig. 1c). However, the activity of POD showed an increase in the TET exposure group compared to the control, even at the lowest concentration (10 μg/L) of TET. Many aromatic compounds can induce the

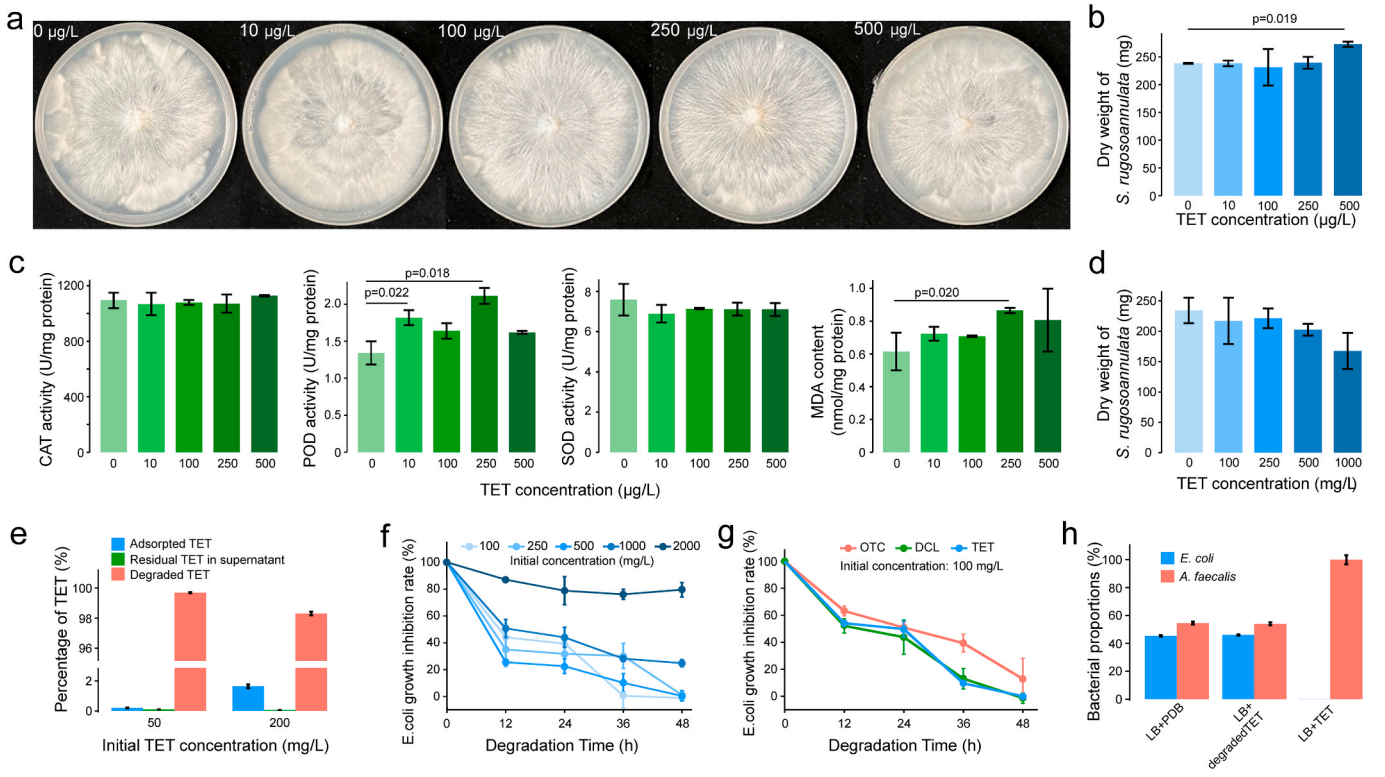

Fig. 1. The impact of TET on *S. rugosoannulata* mycelia and the TET degradation by *S. rugosoannulata*. (a) The impact of different concentrations of TET on the growth of *S. rugosoannulata* mycelia grown on PDA plates. (b, c) The impact of different concentrations of TET on the dry weight, enzymatic activities of CAT, SOD, and POD, and MDA content of submerged cultivated *S. rugosoannulata* mycelia in PDB media.(d) The impact of high concentrations of TET on the dry weight of submerged cultivated *S. rugosoannulata*. (e) Percentage of TET removal by *S. rugosoannulata* mycelia through adsorption and degradation. (f) The inhibitory effects of the TET degradation products on the growth of *E. coli*. (g) The inhibitory effects of the TET, DCL, and OTC degradation products on the growth of *E. coli*. (h) The influence of culture media, TET, and TET degradation products on the growth of mixed TET-susceptible strain *E. coli* and TET-resistant strain *A. faecalis*.

expression of lignin modification enzymes (LMEs), including POD, in white-rot fungi [45–47]. Since TET contains aromatic rings, TET or its aromatic degradation products might induce the expression of POD. CAT and SOD constitute the primary antioxidant enzyme system, and the activity levels of these two enzymes did not rise. We further examined the levels of MDA and found that MDA content significantly increased under TET exposure when the TET concentration exceeded 250 μg/L. MDA content increased by 140.86 % and 131.26 % with 250 μg/L and 500 μg/L of TET, respectively, compared to control. MDA is produced by lipid peroxidation of ROS against the cell membrane.The increased MDA content indicated that the cells were experiencing oxidative stress. Oxidative stress measurement using the ROS indicator 2′,7′-dichlorofluorescin diacetate showed that only a slight amount of ROS was produced in *S. rugosoannulata* mycelia under low concentration of TET (Fig. S1). Although high concentrations of TET are typically not found in natural environments, the impact of high concentrations TET on the mycelial growth of *S. rugosoannulata* was also evaluated for reference. The dry weight was almost similar in treatments with TET concentration of 100 mg/L and 250 mg/L. When the concentration reached 500 mg/L and 1000 mg/L, the dry weight of submerged cultivated *S. rugosoannulata* mycelia decreased by only 13.54 % and 28.51 %, respectively (Fig. 1d). These findings suggest that although environmentally relevant concentrations of TET induce a small amount of ROS production, they do not affect the growth of *S. rugosoannulata*.

To explore how *S. rugosoannulata* mitigates the impact of high concentrations of TET on mycelial growth, the TET concentration in the supernatant of the TET-addition group was measured using HPLC. The results indicate that after eight days of cultivation, TET disappeared from the supernatant. The degradation rates of TET in the supernatant with 50 mg/L and 200 mg/L TET were 99.70 % and 98.31 %, respectively. The adsorption rates of TET in the microspheres of *S. rugosoannulata* with 50 mg/L and 200 mg/L TET were 0.10 % and 0.05 %, respectively (Fig. 1e, Table S3), indicating that the efficient removal of TET by *S. rugosoannulata*. These findings suggest that *S. rugosoannulata* removed TET through biodegradation. The key to antibiotic removal is alleviating the pressure imposed on non-antibiotic-resistant bacteria, and the growth of *E. coli* is commonly used to evaluate the growth inhibition effects of antibiotic degradation products [22,24]. White-rot fungi typically degrade xenobiotics by secreting extracellular enzymes, therefore, we used the supernatant for antibiotic degradation [48]. After 48 h of degradation, up to 500 mg/L of TET could be completely converted to products harmless to *E. coli* (Fig. 1f). When the initial concentrations of TET were 1000 mg/L and 2000 mg/L, after 48 h of degradation, the *E.* coli growth inhibition rate decreased from 100 % to 24.81 % and 79.56 %, respectively (Fig. 1f). DCL and OTC are two tetracycline antibiotics commonly used in animal husbandry. After a 48-hour reaction, 100 mg/L DCL and OTC could also be transformed into non-antibiotic products by the supernatant, indicating that *S. rugosoannulata* can remove not only TET but also other tetracyclines (Fig. 1g). The results suggest that *S. rugosoannulata* can transform TET into non-antibiotic products through biodegradation, and extracellular enzymes are responsible for this process.

The primary issue with antibiotics is that they confer a selective advantage to ARB and promote the mobilization and horizontal transfer of a wide range of ARGs to ARB, particularly those causing disease [2, 49]. Hence, it is imperative to ascertain whether the TET degradation products by *S. rugosoannulata* confer a growth advantage to TET-resistant strains. A TET-resistant strain *A. faecalis* and TET-sensitive *E. coli* cells were inoculated into LB media supplemented with PDB-cultivated *S. rugosoannulata* supernatant. After 24 h of cultivation,

E. coli and *A. faecalis* accounted for 45.42 % and 54.57 % of the cell population(Fig. 1h, Fig. S2), respectively, indicating similar growth capacities of both strains in the absence of selective pressure. After the addition of 50 mg/L of TET, the final $OD_{600\ nm}$ value decreased from the control's 2.44 to 1.11 (Fig. S2), with a significant change in bacterial proportions. *E. coli* accounted for only 0.046 %, while *A. faecalis* comprised 99.95 % (Fig. 1h), indicating that TET provides a growth advantage to *A. faecalis*. Upon supplementation with TET degradation products by *S. rugosoannulata*, rather than intact TET, in the culture medium, the cell population of *A. faecalis* returned to 53.98 % (Fig. 1h). These results indicate that TET products after degradation by *S. rugosoannulata* did not provide a growth advantage to TET-resistant strains, thereby not contributing to the spread of ARB and ARGs.

3.2. Exploring of enzymes responsible for antibiotics degradation

Most of the secreted oxidoreductases of white-rot fungi are inducible enzymes [50]. To investigate whether TET degradation enzymes are also inducible, we used different media (PDB and MYN) to induce the expression of these enzymes. The TET degradation efficiency of the secreted proteins was determined based on the *E. coli* inhibition rate. After 48 h of degradation, the inhibition rate of TET degradation products by the supernatant of PDB and MYN media was 1.18 %, and 88.02 %, respectively (Fig. 2a). The supernatants of *S. rugosoannulata* GL0170 cultivated in PDB and MYN did not inhibit the growth of *E. coli* in the absence of TET (Fig. S3), indicating that TET-degrading enzymes had higher expression levels in PDB media compared to those in MYN media.

Laccase and peroxidase are the primary enzymes in the supernatant of fungi responsible for the degradation of xenobiotics, including antibiotics [48]. The ligninolytic enzyme systems from *T. versicolor* can synergistically degrade Azure B and sulfanilamide antibiotics [51]. Immobilized laccase from *Cerrena* was used for TET degradation by Yang et al. [52]. Weng et al. reported that laccase-mediator systems (LMS) could oxidize two SAs, sulfadimethoxine and sulfamonomethoxine [53]. Peroxidase-catalyzed reactions require H_2O_2 as a substrate [54]. Given that antibiotics could be degraded by the supernatant of *S. rugosoannulata* in the absence of added H_2O_2, we tested whether laccases in the supernatant were responsible for the degradation of TET and other antibiotics. Enzyme activity assays revealed that laccase activities in the supernatant of PDB media were 15.26-fold and 7.84-fold those of laccase activities in the MYN supernatant on day 6 and day 8, respectively (Fig. 2b). Zhang et al. reported that adding Azure B dye and sulfacetamide to the medium could promote the activity of corresponding degrading enzymes in *T. versicolor* WH21 [51]. The above results also suggested that TET might induce the expression of guaiacol oxidase. Therefore, 50 mg/L TET was added to the PDB and MYN media on day 6. The addition of TET increased the laccase activity in the supernatant of both PDB and MYN media by 7.20-fold and 3.03-fold, respectively. These results suggest that laccases were responsible for TET degradation in the secretome of *S. rugosoannulata*. It also confirms that the increase of POD activity under TET exposure was due to the induction of oxidase expression rather than an oxidative stress response.

To explore the enzymes involved in TET degradation, a label-free quantitative proteomic approach was performed to analyze the secretome of *S. rugosoannulata* in different media. A total of 360 proteins were identified in 9 protein samples, with 259, 315, and 130 proteins identified in the PDB, PDBT, and MYN groups, respectively (Fig. 2c, Table S4). The PDB and PDBT groups shared more proteins (244) than those between the PDB and MYN groups (90) and the PDBT and MYN groups (97). The principal component analysis (PCA) exhibited similar results, as shown in Fig. 2d. There were significant differences between the MYN group and the other two groups, indicating that the protein secretion pattern of the MYN group was significantly different from that of the other two groups. Laccases belong to the auxiliary activities (AA) class within the carbohydrate-active enzymes (CAZymes). A total of 151 CAZymes were identified in the three groups, with 110, 133, and 54 detected in the PDB, PDBT, and MYN groups, respectively (Fig. 2e).

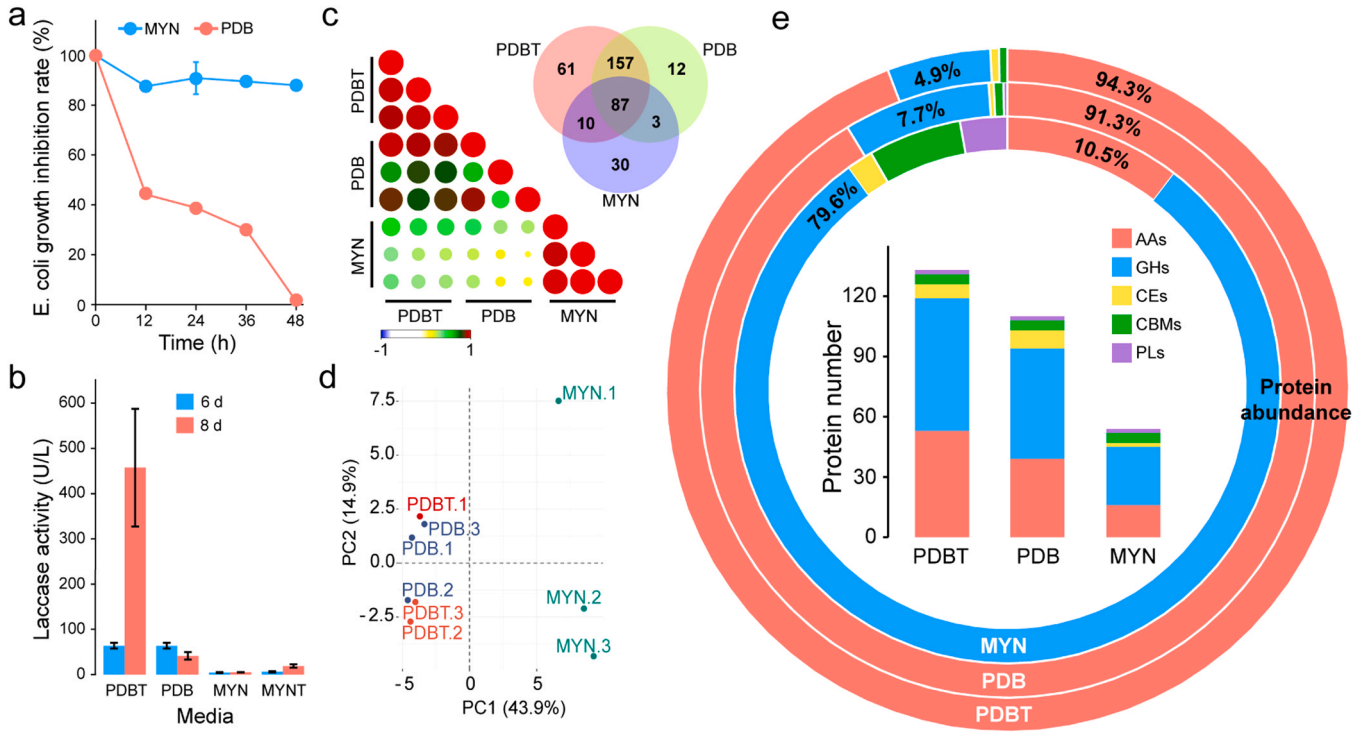

Fig. 2. Proteomic analysis of *S. rugosoannulata* secretome with different TET degradation capacities. (a) The influence of TET degradation by *S. rugosoannulata* culture supernatant in different media on the inhibition rate of *E. coli* growth. (b) The laccase activity of *S. rugosoannulata* culture supernatant in different media with and without TET induction. (c) Venn diagram and Pearson correlation analysis of the proteome from three groups. (d) PCA of the secretome of *S. rugosoannulata* in various media. (e) The identified protein numbers and abundance of CAZyme proteins among the secreted proteins of *S. rugosoannulata*.

Among the identified CAZymes, the numbers of enzymes from the AA family in the PDB, PDBT, and MYN groups were 39, 53, and 16, respectively (Fig. 2e). In contrast to the detected protein numbers, protein abundance belonging to the AA family accounted for 91.3 % and 94.3 % of the total CAZyme abundance in the PDB and PDBT groups, respectively. However, AA family enzymes only accounted for 10.5 % of the total CAZyme abundance in the MYN group. These results indicate that proteins from AA families are more represented in the PDB and PDBT groups compared to the MYN group.

Six putative laccases from the AA1 family were identified in all three samples (Table S5), which were assumed to be responsible for the antibiotic degradation in *S. rugosoannulata*. The expression abundance of these laccases is shown in the heat map in Fig. S4. The expression of five laccases (MDBSrug1_05167, MDBSrug1_06559, MDBSrug1_07931, MDBSrug1_02750, and MDBSrug1_05008) was significantly higher in the PDB and/or PDBT groups than in the MYN group. Sequence alignment showed that MDBSrug1_00049 has the highest sequence similarity (61.99 %) to the functionally validated antibiotic-degrading laccase

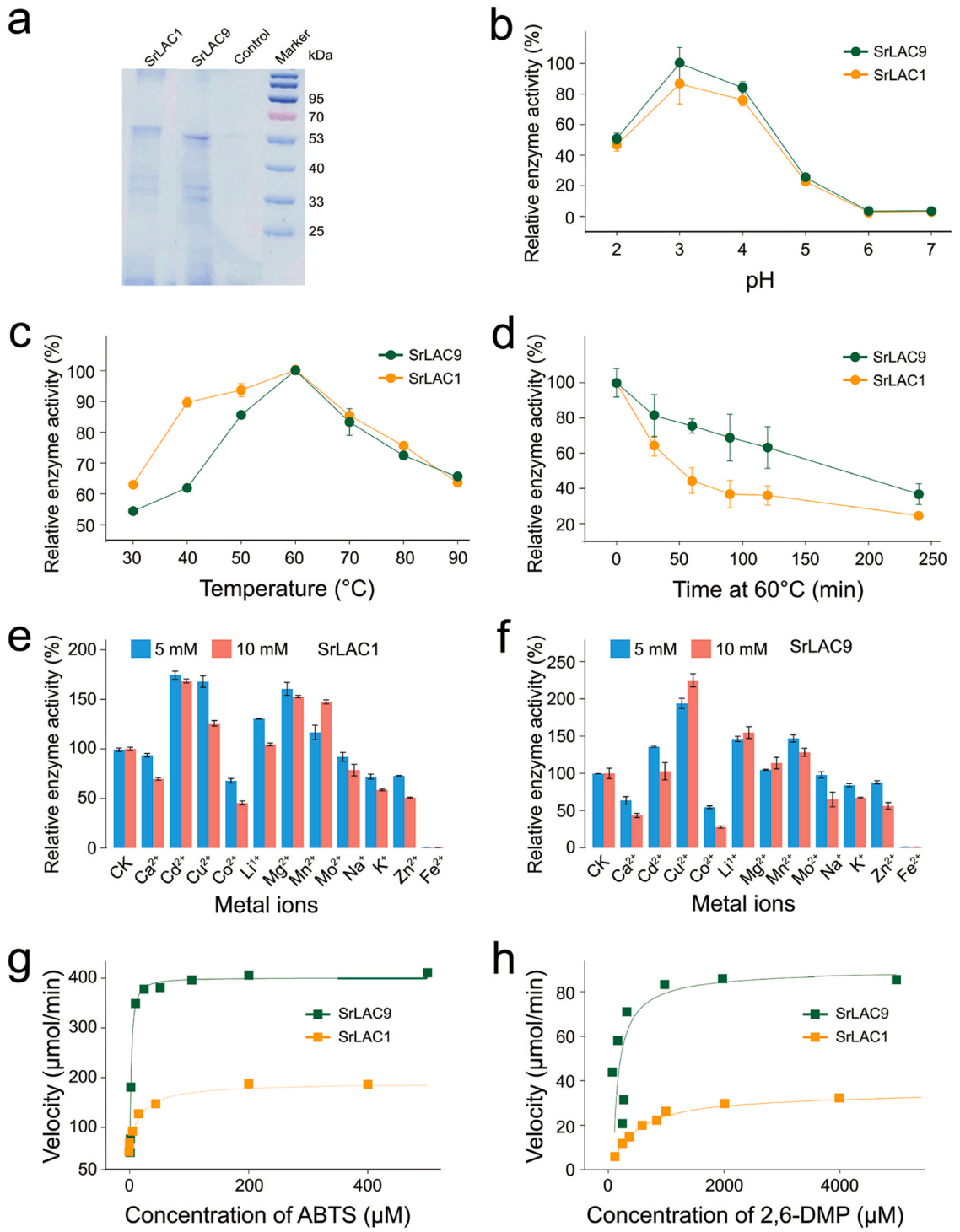

Fig. 3. Catalytic characteristics of purified SrLAC1 and SrLAC9. (a) SDS-PAGE of purified SrLAC1 and SrLAC9. (b, c) Effect of pH and temperature on the relative enzyme activity of SrLAC1 and SrLAC9. (d) Temperature stability of SrLAC1 and SrLAC9. (e, f) Effect of metal ions on the relative enzyme activity of SrLAC1 and SrLAC9. (g) Kinetic studies of ABTS for SrLAC1 and SrLAC9. (h) Kinetic studies of 2,6-DMP for SrLAC1 and SrLAC9.

BAD98306.1 [34]. Therefore, the two laccases (MDBSrug1_05167 and MDBSrug1_07931) with the highest abundance in the PDBT group, and the laccase MDBSrug1_00049, with the highest sequence similarity to BAD98306, were selected for subsequent antibiotic degradation studies.

3.3. Heterologous expression and catalytic properties of SrLAC1 and SrLAC9

To validate the function of the laccases, they were heterologously expressed. Given the potential glycosylation modification of laccases in white-rot fungi, *P. pastoris* was chosen as the host cell for heterologous expression in this study instead of *E. coli*. The expression conditions were optimized (Fig. S5), and heterologously expressed His-tagged recombinant laccases were purified by Ni-affinity chromatography. Two laccases, MDBSrug1_07931 (SrLAC9) and MDBSrug1_00049 (SrLAC1), exhibited laccase activity (Table S6). The sequence similarity between these two laccases is 73.37 %. SDS-PAGE analysis revealed characteristic protein bands around 58 kDa and 56 kDa (Fig. 3a), consistent with their theoretical molecular weights. These molecular weights are similar to those of laccases from *Bacillus velezensis* (58 kDa) [55] and *Pycnoporus sp.* SYBC-L10 (60 kDa) [25]. SrLAC1 and SrLAC9 had exhibited optimal enzyme activity at pH 3.0 (Fig. 3b). Above pH 5.0, their oxidizing activity towards ABTS was lost, indicating their activity in acidic conditions. The optimal temperature for SrLAC1 and SrLAC9 was 60 ℃ (Fig. 3c), with retained ABTS oxidizing activity at 90 °C of 63.72 % and 65.51 %, respectively. SrLAC1 and SrLAC9 demonstrated heat resistance, which was speculated to be related to the content of alanine, proline, and valine amino acids in the protein (Table S7) [34]. Thermal stability at 60 °C showed that after 0.5 h, approximately 64.02 % and 81.26 % of the original enzyme activity remained in SrLAC1 and SrLAC9, respectively (Fig. 3d). SrLAC1 and SrLAC9 exhibited higher thermal stability compared to LeLac, a laccase from another mushroom, *Lentinula edodes* [56].

The effects of metal ions on the activity of SrLAC1 and SrLAC9 were investigated by adding final concentrations of 5 mM or 10 mM ions into the reaction mixture. Cd^{2+}, Cu^{2+}, Li^{+}, Mg^{2+}, and Mn^{2+} promoted the activity of SrLAC1 and SrLAC9. SrLAC1 showed higher activity enhancement with 5 mM Cu^{2+} compared to 10 mM Cu^{2+}, consistent with a previous study [57]. Ca^{2+}, Co^{2+}, Na^{+}, K^{+}, and Zn^{2+} ions inhibited the activity of SrLAC1 and SrLAC9. Fe^{2+} strongly inhibited the activity of both enzymes (Fig. 3ef). This inhibition may be attributed to Fe^{2+} ion-mediated reduction of $ABTS^{+}$ to the ABTS [58]. The effect of metal ions on SrLAC1 activity aligned closely with previous reports on laccases, whereas SrLAC9 exhibited different responses, indicating structural and functional differences between these two enzymes. Additionally, SrLAC1 and SrLAC9 demonstrated strong resistance to organic solvents, as detailed in Table S8. Methanol, ethanol, acetonitrile, acetone, and trichloromethane at 30 %(v/v) concentration significantly inhibited SrLAC1 and SrLAC9 activity, with inhibition rates exceeding 80 %. EDTA and SDS slightly inhibited the activity of SrLAC1 and SrLAC9.

The catalytic efficiency and substrate affinity of ABTS and 2,6-DMP were assessed. For SrLAC1 in 50 mM malonic acid buffer at pH 3.0 and 60 °C, the apparent K_m and k_{cat} values for ABTS were 19.92 μM and 1222.57 s^{-1}, respectively (Fig. 3g). For 2,6-DMP, the apparent K_m and k_{cat} values for SrLAC1 were 115.41 μM and 260.79 s^{-1}, respectively (Fig. 3h). SrLAC9 exhibited apparent K_m and k_{cat} values of 2.52 μM and 1742.15 s^{-1}, respectively, for ABTS (Figs. 3g), and 98.93 μM and 394.91 s^{-1}, respectively, for 2,6-DMP (Fig. 3h). These results indicate that SrLAC1 and SrLAC9 displayed higher affinity towards ABTS compared to 2,6-DMP. Both laccases, SrLAC1 and SrLAC9, were successfully expressed and purified from *P. pastoris* cells and their activity were verified in vitro. These findings provide valuable insights for research on antibiotics and lignocellulose degradation.

3.4. TET degradation by SrLAC1 and SrLAC9

After 180 min of degradation, TET degradation efficiencies without mediators were only 6.40 % and 10.53 % for SrLAC1 and SrLAC9, respectively (Fig. 4a). These results demonstrate that both laccases were capable of degrading TET, while the low degradation possibly due to the absence of mediators. Laccases are oxidases with redox potentials typically below 800 mV, enabling them to oxidize phenolic substrates with low redox potentials. However, oxidation of non-phenolic substrates, which can have redox potentials up to 1500 mV, is more challenging. Previous studies have shown that mediators play a crucial role in enhancing the degradation of antibiotics through laccase-mediated oxidation [59]. According to a commonly proposed reaction model, when laccase cannot directly act on substrates, it can initially oxidize an intermediary molecule, known as the mediator, to generate active free radicals. These radicals then react with the substrate [60]. Therefore, mediators were introduced into the reaction system to form laccase-mediator systems (LMS), overcoming the inertness of non-phenolic substrates. The degradation capacities of TET by the two laccases were evaluated using widely used mediators HBT and ABTS, as well as the lignin-derived mediator SyA, at concentration ranging from 0.2 mM to 2 mM (Fig. S6). ABTS is oxidized by laccase to $ABTS^{+}$, which is further oxidized to $ABTS^{2+}$. $ABTS^{2+}$, with a high redox potential capable of directly attacking non-phenolic substrates [61]. HBT is oxidized by laccase to form HBT^{+}• radicals, which is deprotonated to form N-O• radicals attacking the substrates [62]. Methoxy groups in SyA decrease redox potentials and increase electron density at the phenoxy group, which allowed these compounds to be easily oxidized by laccases [63].

Compared to individual laccases, the TET degradation efficiency of the LME systems was significantly enhanced (Fig. 4a). At a mediator concentration of 1 mM, the addition of HBT, ABTS, and SyA resulted in TET degradation efficiencies of 73.75 %, 99.89 %, and 99.46 % for SrLAC1, respectively, and 92.62 %, 99.22 %, and 90.66 % for SrLAC9, respectively. In subsequent reactions, the laccase/ABTS system nearly completely degrade TET at concentrations ranging from 25–400 mg/L within 180 min, demonstrating high efficiency in TET degradation (Fig. 4b). Suda et al. reported that the laccase-HBT system could completely degrade 10^{-4} M TET within 1 h, which is similar to the performance of the SrLAC9-HBT system [24]. The efficiency of TET degradation varied with HBT concentration, increasing from 0.2 mM to 1 mM HBT enhanced TET degradation, but further increasing to 2 mM HBT decreased efficiency (Fig. S6). In contrast, varying concentrations of ABTS and SyA had minimal impact on TET degradation within the tested range (Fig. S6). Ouyang et al. indicated that using a laccase from a *Lysinibacillus* bacterium, the laccase-ABTS system exhibited significantly higher TET degradation capacity compared to the laccase-SyA system [64]. Tian et al. reported similar results, where the Lac-Q-ABTS system showed the highest degradation rates, with 96 % removal of TET and 90 % removal of OTC after a 3-minute incubation at 25 °C (pH 6.0). In contrast, the Lac-Q-SyA system achieved only 49 % removal of TET and 45 % removal of OTC [65]. In our study, both ABTS and SyA mediators achieved high degradation efficiencies (> 90 %) (Fig. 4a), possibly because SyA, as a lignin degradation product, is readily accessible as a mediator for *S. rugosoannulata*. Additionally, SyA was found to induce the expression of laccase in *S. rugosoannulata* (data not shown). These results suggest that SrLAC1 and SrLAC9 preferentially utilize ABTS and SyA as mediators for TET degradation.

To confirm their structural similarity to laccases, three-dimensional models of SrLAC1 and SrLAC9 were generated using homology modelling (Fig. 4c). Sequence analysis revealed that SrLAC1 and SrLAC9 each contain four Cu atoms organized into an active site [66], which serves as a catalytic backbone for the catalysis of substrates. All fungal laccases exhibit a conserved architecture comprising three domains arranged in a β-barrel structure. SrLAC1 consists of three domains: domain1 (51−153), domain2 (166−327), domain3 (395−518), while SrLAC9

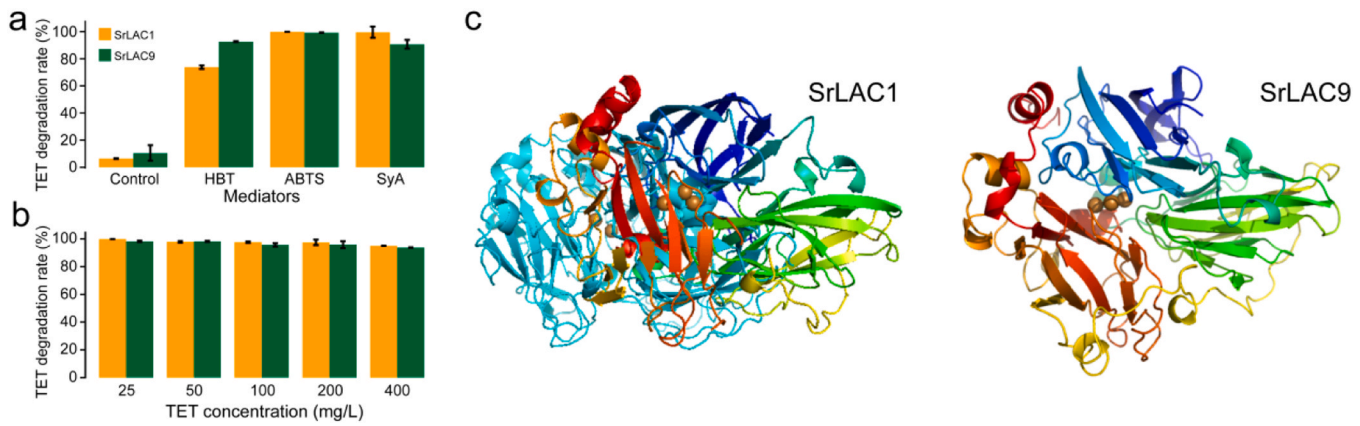

Fig. 4. TET degradation by SrLAC1 or SrLAC9 and the predicted models of laccases. (a) The impact of mediators on the degradation of TET by SrLAC1 or SrLAC9. (b) The degradation efficiency of SrLAC1 or SrLAC9 with different TET concentrations. (c) Homologous modeling of SrLAC1 and SrLAC9.

also comprises three domains: domain1 (50−150), domain2 (163−305), and domain3 (372−494). Laccase sequences typically feature four characteristic regions (L1-L4) [67]. Comparison of these characteristic regions and copper ion binding sites of SrLAC1 and SrLAC9 with other laccases is shown in Fig. S7, indicating that SrLAC1 and SrLAC9 are conserved fungal laccase enzymes.

3.5. Degradation of multiple antibiotics

The antibiotic detection rates in the soils and surface water of eastern and southeastern provinces of China are reported to be very high [44]. Generally, multiple antibiotics are often simultaneously detected in contaminated environments [44,68]. Residule of multiple antibiotics in compost, soil, and surface runoff could potentially impact *S. rugosoannulata* production. Among these, TCs and QNs, and SAs were the most frequently detected antibiotics [15,44,69,70]. Therefore, the degradation capacity of eleven commonly used antibiotics from TCs, QNs, and SAs by *S. rugosoannulata* and two laccases was evaluated. The inhibitory concentrations of different antibiotics against *E. coli* were determined, and concentrations that completely inhibited the growth of *E. coli* were used in subsequent experiments. Specifically, the concentration of TCs was 1 mg/L, the concentration of SAs was 120 mg/L, and the concentration of QNs was 1 mg/L (Table S9, Fig. 5a). To assess the degradation of multiple antibiotics by *S. rugosoannulata* and the

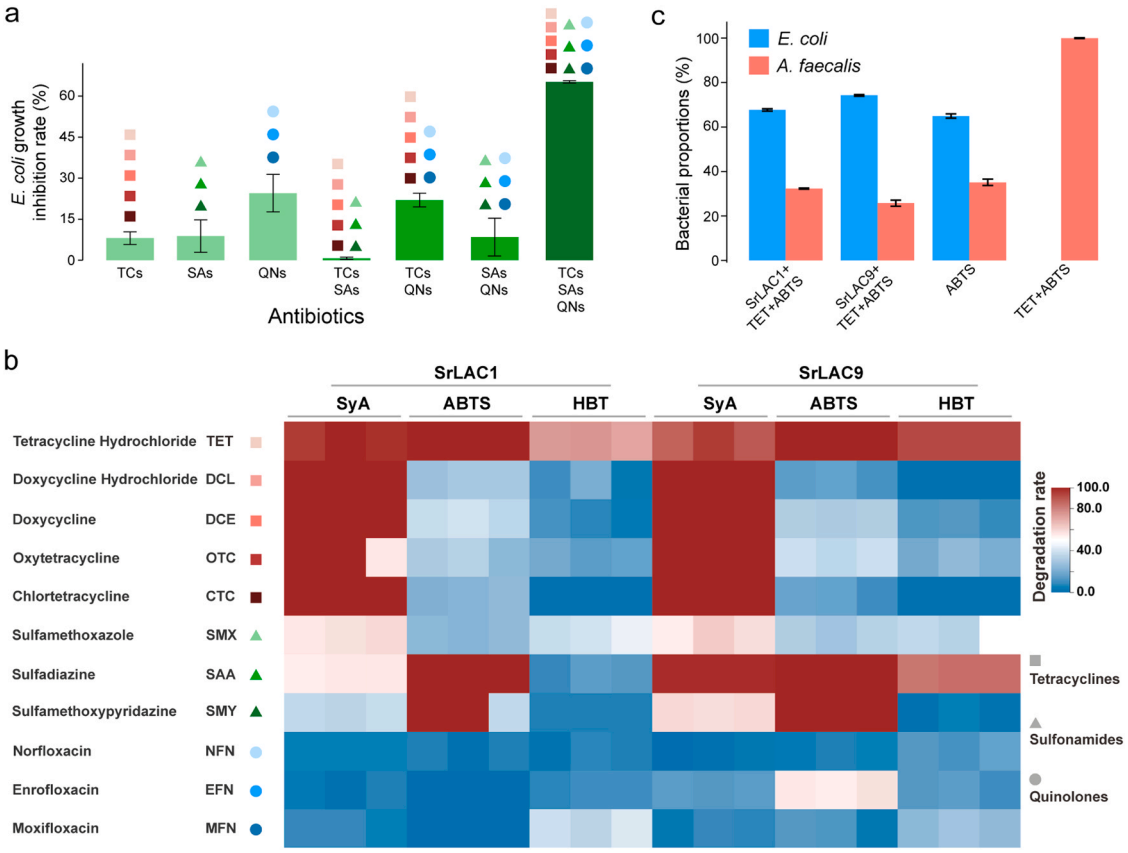

Fig. 5. Multiple antibiotics degradation by *S. rugosoannulata* and two purified laccases. (a) Degradation of eleven mixed antibiotics from TCs, SAs, and QNs by the culture supernatant of *S. rugosoannulata*. (b) A heat map illustrating the degradation of 11 antibiotics by SrLAC1 and SrLAC9 in the presence of three different mediators. (c) The effects of TET and TET degradation products by SrLAC1 and SrLAC9 on the growth of *E. coli* and TET-resistant strain *A. faecalis*.

synergistic effects among them, TCs, SAs, and QNs were mixed in various combinations as indicated in Table S9 and degraded using the supernatant of *S. rugosoannulata* culture for 48 h. The growth of *E. coli* was used to evaluate the antibiotic degradation efficiency of *S. rugosoannulata*. Results showed that when TCs and SAs mixtures were degraded individually, the growth inhibition rates of *E. coli* were 8.07 % and 8.81 % (Fig. 5a), respectively. However, when TCs and SAs mixtures were simultaneously added to the same reaction system, the growth inhibition rate of *E. coli* decreased to 0.71 % (Fig. 5a), suggesting a synergistic degradation effect between TCs and SAs. In contrast, the degradation products of QNs mixture resulted in a 24.52 % growth inhibition rate *of E. coli* (Fig. 5a), indicating a lower degradation efficiency of *S. rugosoannulata* for QNs compared to TCs and SAs. Furthermore, the degradation products of TCs + QNs mixture showed a similar growth inhibition rate to QNs alone, at 22.00 % (Fig. 5a). However, the degradation products of SAs + QNs mixture exhibited a decreased growth inhibition rate to 8.43 % (Fig. 5a), suggesting a synergistic degradation effect between SAs and QNs. It is speculated that the degradation products of SAs act as efficient mediators for the degradation of the other two classes of antibiotics. When all three classes of antibiotics were combined for degradation, the growth inhibition rate of *E. coli* by the degradation products reached 65.22 % (Fig. 5a), indicating that the antibiotic concentration was too high and exceeded the degradation capacity of the supernatant. Overall, *S. rugosoannulata* demonstrates high efficiency in degrading multiple mixed antibiotics, with a notably higher capacity observed for TCs and SAs compared to QNs.

The antibiotic substrate spectra of purified SrLAC1 and SrLAC9 were determined using HPLC analysis with eleven antibiotics from TCs, SAs, and QNs as substrates. Degradation reactions were conducted with 0.5 U of laccase, 1 mM mediator, and 50 mg/L of antibiotic substrate for 3 h at 30 °C. Three LMS setups exhibited significant differences in the degradation of TCs antibiotics (with the exception of TET). Specifically, the laccase-SyA system demonstrated the highest degradation efficiency, exceeding 90 % for all TCs. In contrast, the degradation efficiencies of the other two systems for TCs (excluding TET) remained below 40 % (Fig. 5b, Fig. S8). Additionally, the degradation efficiencies of the laccase-ABTS system surpassed those of the laccase-HBT system for the degradation of all TCs except TET. This contrasts with the findings of Suda et al. [24], who reported complete degradation of TCs by a laccase from *T. versicolor* in the Lac-HBT system. Our results indicate that SrLAC1 and SrLAC9 efficiently degrade TCs, with SyA proving to be the superior mediator for TCs oxidation.

Similar to the degradation of TCs, the efficiency of SMX degradation was highest when SyA was used as the mediator, achieving 57.93 ± 1.08 % and 58.38 ± 2.87 % degradation for SrLAC1 and SrLAC9, respectively. Following this, HBT as the mediator showed degradation efficiencies of 40.35 ± 2.57 % and 39.85 ± 5.81 % for SrLAC1 and SrLAC9, respectively, while ABTS exhibited the lowest degradation efficiency (Fig. 5b, Fig. S9). Yang et al. [55] reported similar findings, showing faster SMX oxidation in the presence of SyA compared to ABTS. The immobilized laccase from *Echinodonitium taxodii* favored syringic acid over HBT as the mediator for SMX oxidation, achieving over 95 % degradation within 30 min at a laccase concentration of 0.2 U/mL [71]. In contrast, studies by Yang et al. indicated varied results where ABTS mediated the highest SMX degradation efficiency among several bacterial laccases, with SyA showing a minor inhibitory effect on SAs removal [55]. Given that SyA is more accessible to fungi than bacteria, fungal laccases may have evolved to effectively utilize SyA as a mediator. When ABTS was employed as the mediator, both SrLAC1 and SrLAC9 achieved 100 % degradation rates for SAA and SMY. Subsequently, degradation rates using SyA as the mediator were significantly higher than those using HBT. Specifically, with SyA as the mediator, SrLAC1 and SrLAC9 achieved degradation rates of 55.74 ± 0.85 % and 98.33 ± 0.20 %, respectively, for SAA, and 36.16 ± 0.85 % and 58.83 ± 0.39 %, respectively, for SMY (Fig. 5b). Previous research using the strain EcN-IL, which displays surface-bound laccase, achieved a SAA degradation efficiency of 37 ± 1 % within 3 h at a laccase activity of 2 ± 1 U/mg dry weight of cells [72], which is lower than that in our study. SMY, widely used in livestock production, had not been previously reported for laccase degradation. In our study, SrLAC1 and SrLAC9 completely removed SMY within 3 h, suggesting a promising approach for SMY removal.

Zou et al. reported a 93.7 % degradation rate of NFN using magnetically modified biochar immobilized laccase in the presence of ABTS after 48 h [25], while Blánquez et al. demonstrated that the SilA-acetosyringone system from *Streptomyces ipomoeae* degraded over 90 % of NFN [73]. Immobilized laccases from *T. versicolor* achieved 77.0 % and 75 % degradation of MFN as reported by Zou et al. and Vojdanitalab et al., respectively [25,74]. Additionally, this immobilized laccase effectively removed 98 % of EFN after 6 h in the presence of HBT, and 65.4 % of EFN with 1 mM ABTS at pH 4 after 48 h of degradation [25,75]. However, in our study, the degradation efficiency of QNs is notably lower compared to TCs and SAs. The highest degradation efficiency observed for QNs was when ABTS was used as the mediator, achieving a degradation efficiency of 55.80 ± 0.87 % for EFN by SrLAC9, while none of the other QNs reached efficiencies higher than 40 %. In contrast to TCs and SAs degradation, HBT appears to be a more suitable mediator for some QNs. Using HBT as the mediator, SrLAC9 achieved the highest degradation efficiency for NFN at 14.15 ± 0.78 %, and SrLAC1 achieved the highest for MFN at 37.84 ± 2.56 % (Fig. 5b, Fig. S9, Table S10). It is evident that the degradation efficiency of SrLAC1 and SrLAC9 for QNs is lower compared to the laccase from *T. versicolor*. Nonetheless, these results are consistent with those obtained using crude enzymes from the supernatant of *S. rugosoannulata* culture (Fig. 5b), which also showed lower degradation efficiency for QNs.

The impact of TET and its degradation products by SrLAC1 and SrLAC9 on the growth of TET-sensitive *E. coli* and TET- resistant *A. faecalis* strains was assessed. It was found that the degradation products of TET did not provide a growth advantage to the TET-resistance strain (Fig. 5c), consistent with above results using crude enzymes (Fig. 1h). Overall, SrLAC1 and SrLAC9 demonstrated similar antibiotic degradation capabilities across the three antibiotics classes as observed with the supernatant of *S. rugosoannulata* culture, affirming their role in antibiotic degradation within the secreted proteins of *S. rugosoannulata*. The catalytic efficiency of both laccases was generally comparable across most antibiotics, with enhanced degradation efficiency typically observed when SyA was employed as the mediator. SyA, derived from lignin syringyl units [76], likely produced during the growth of *S. rugosoannulata* on lignocellulosic substrates. This finding holds significant implications for antibiotic degradation during the cultivation of *S. rugosoannulata* for commercial purposes.

3.6. Identification and risk assessment of antibiotics degradation products

In order to explore the degradation pathways of SrLAC1 and SrLAC9 on TET, DCL, and SAA, UPLC-MS/MS was used to identify the degradation products. Based on antibiotic structures and existing literatures [33,77,78], the pathways of SrLAC1 and SrLAC9 for degrading TET, DCL, and SAA were elucidated. A total of 13 metabolic intermediates of TET were detected, with their mass spectrometry data and possible chemical formulas detailed in Table S11 and depicted in Fig. 6. Seven distinct metabolic pathways were identified for SrLAC1 and SrLAC9 in TET degradation, as illustrated in Fig. 6a. In pathway 1, TET was hydroxylated to generate TET1 (m/z 459.15491), followed by carboxylation to TET2 (m/z 457.12482), subsequent demethylation to TET3 (m/z 429.15033), oxidation to TET4 (m/z 415.20755), and deamination yielding TET5 (m/z 400.13965). In pathway 3, TET undergoes oxidation to TET3, followed by further oxidation to TET4 and deamination to form TET5. In pathway 4, TET was demethylated to TET7 (m/z 429.15027) and TET8 (m/z 413.11252), followed by deamination to generate TET9 (m/z 398.08315), and subsequent conversion to TET10 (m/z

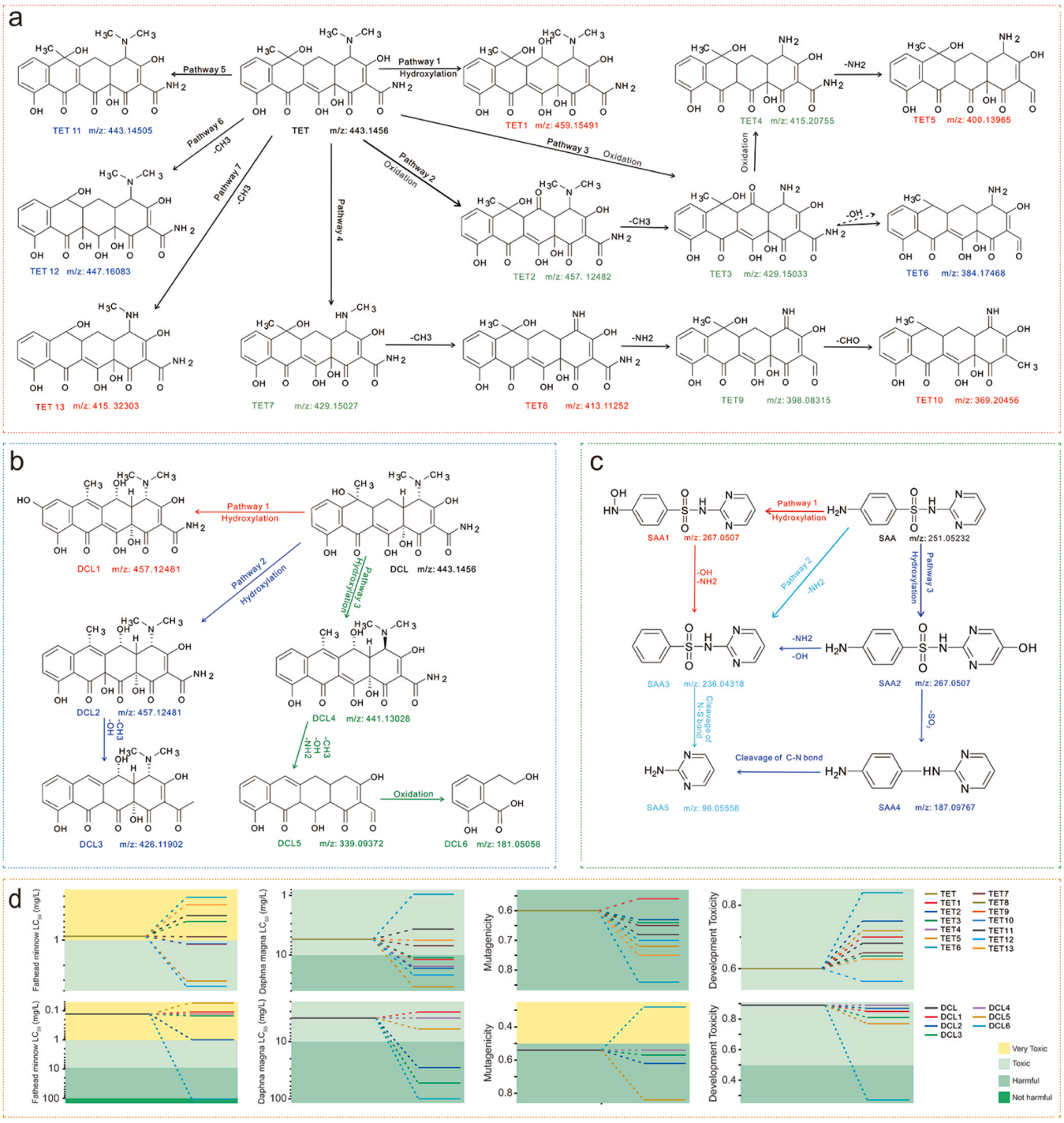

Fig. 6. Proposed degradation pathways of antibiotics by two laccases and the safety assessment of degradation metabolites. (a-c) Degradation pathways of TET (a), DCL (b), and SAA (c) by SrLAC1 and SrLAC9. (d) Safety assessment of TET, DCL, and their degradation products in terms of fathead minnows (LC50 96 hr), *Daphnia magna* (LC50 48 hr), mutagenicity, and developmental toxicity.

369.20456). In pathway 7, the direct demethylation on the benzene ring of TET, resulting in the formation of TET13 (*m/z* 415.32303). SrLAC1 and SrLAC9 exhibit different pathways in the degradation of TET. For SrLAC9, three distinct metabolic pathways were identified. In pathway 2, TET undergoes oxidation to TET2, followed by demethylation to TET3, and further dehydroxylation leading to TET6 (*m/z* 384.17468). In pathway 5, the direct oxidizing on the benzene ring of TET leads to the formation of TET11 (*m/z* 443.14505). In pathway 6, the direct demethylation on the benzene ring of TET, leading to the formation of TET12 (*m/z* 447.16083).

In this study, six metabolic intermediates of DCL were detected using mass spectrometry, with their corresponding chemical formulas detailed in Table S11 and depicted in Fig. 6b. The degradation pathways of DCL by SrLAC1 and SrLAC9 were found to be consistent, revealing three possible pathways. In pathway 1, DCL undergoes hydroxylation to yield DCL1 (*m/z* 457.12481) [79]. In pathway 2, Oxidation and cleavage of the double bond in DCL occur, with subsequent oxidation of the hydroxyl group to a carbonyl, resulting in DCL2 (*m/z* 457.12481) [80]. Further demethylation and deamination lead to the formation of DCL3 (*m/z* 426.11902). In pathway 3, structural transformation of DCL results

in the formation of DCL4 (*m/z* 441.13028), followed by demethylation, formation of amino and hydroxyl groups to yiled DCL5 (*m/z* 339.09372), and further experienced an oxidation reactions to yield DCL6 (*m/z* 181.05056) [32]. It is speculated that CO_2 and H_2O are produced in these pathways [81].

Five major transformation products of SAA were identified in both SrLAC1 and SrLAC9 reaction mixtures, with their mass spectra data detailed in Table S11, and speculated pathways for SAA degradation by the two laccase enzymes are depicted in Fig. 6c. Similar transformation products have also been identified as described in some previous studies [34,82,83]. SAA undergoes hydroxylation to generate SAA1 (*m/z* 267.0507) or SAA2 (*m/z* 267.0507). SAA2 was a hydroxylated intermediate in the degradation process of SAA [83]. SAA1 and SAA2 can lose amino and hydroxyl groups to form SAA3 (*m/z* 236.04318), and then C-N bond cleavages to form SAA5 (*m/z* 96.05558). SAA2 undergoes sulfur removal to form SAA4 (*m/z* 187.09767), and then C-N bond cleavages to form SAA5 [84]. SAA2 could also lost amino and hydroxyl groups to form SAA3 [84]. The degradation of SAA by SrLAC1 and SrLAC9 primarily involves breaking the C-N bond within the heterocyclic rings, resulting in the production of simpler metabolites [74].

The fathead minnow (96 hr), *Daphnia magna* (48 hr), mutugenicity and developmental toxicity of TET, DCL and their corresponding intermediates were assessed using the Toxicity Estimation Software Tool (TEST) [85,86]. According to Fig. 6d, the LC_{50} values for fathead minnow exposed to TET, DCL, TET3, TET4, TET6, TET7, TET11, TET13, and DCL1–5 were classified as "very toxic". Conversely, intermediates TET1, TET2, TET12, and TET9 were classified as "toxic", and DCL6 was classified as "Not Harmful", indicating a gradual decrease in toxicity among these intermediates. For *Daphnia magna*, as shown in Fig. 6d, the LC_{50} values for TET1, TET2, TET3, TET4, TET5, TET9, TET12, DCL2, DCL3, and DCL6 were higher than those for TET and DCL, with most intermediates considered "harmful". Additionally, the mutagenicity of the intermediates, exclusive of DCL5, was categorized as "Harmful". The developmental toxicity was significantly reduced among the intermediates, with DCL6 also classified as "Harmful" (Fig. 6d). TET8, TET9, and TET10 exhibited no toxic effects on mutagenicity, fathead minnow, or *Daphnia magna*, confirming that the biodegradation of TET and DCL by SrLAC1 and SrLAC9 effectively meets the actual needs of ecological and food safety requirements.

3.7. Distribution of ARGs in commercially produced *S. rugosoannulata* in China

Although the above results have demonstrated that *S. rugosoannulata* can degrade various antibiotics through secreted laccases, effectively eliminating the growth advantage conferred by antibiotics on ARB, it remains unclear whether this antibiotic degradation ability will eliminate the threat posed by ARB and ARGs to the fruiting bodies of *S. rugosoannulata* in practical production. To clarify this, ARGs on the commercially produced fruiting bodies of *S. rugosoannulata* from our lab in Shandong Province and from six other provinces in China (Beijing, Henan, Anhui, Sichuan, Chongqing, and Yunnan) were detected (Fig. 7). Fifty commonly detectable ARGs (Table S12) in compost were selected according to a previous study [17], and only genes with Ct values less than 31 and correct sequences after sequencing were considered positive [43]. According to this standard, none of the seven groups of samples showed the presence of all 50 ARGs. This indicates that the robust antibiotic degradation capability inherent in *S. rugosoannulata* can indeed reduce and eliminate the contamination of ARB and ARGs in the fruiting bodies, thus ensuring the safety of *S. rugosoannulata*.

4. Conclusion

This study explored the potential effects of antibiotics on the straw-rotting mushroom, *S. rugosoannulata*. Our findings reveal that exposure to detectable levels of TET in the environment (<500 μg/L) does not impact the growth of *S. rugosoannulata*, which is due to that *S. rugosoannulata* has the capability to remove TET through

Fig. 7. Spatial distributions of selected antibiotics in *S. rugosoannulata* fruiting body across China.

biodegradation. Importantly, the degradation products of TET no longer inhibit *E. coli* growth or confer a growth advantage to TET-resistant bacteria, thus impeding the spread of ARB and ARGs. *S. rugosoannulata* degrades not only TCs but also antibiotics belonging to the SAs and QNs classes. Laccases in the culture supernatant are responsible for the degradation of these antibiotics, and two laccases, SrLAC1 and SrLAC9, were heterologously expressed, purified, and characterized. Furthermore, none of the *S. rugosoannulata* fruiting bodies from seven provinces in China contain detectable ARGs, confirming our conclusion that *S. rugosoannulata* can convert antibiotics into non-toxic and non-bactericidal products, ensuring the food safety of its fruiting bodies. Overall, this study offers insights into the intrinsic molecular mechanisms ensuring mushroom production safety against antibiotic pollution.

Environmental implication

This research provides new insights into the interaction between mushrooms and their environment. Food safety is a primary concern in the edible mushroom industry. Straw-rotting mushrooms, such as *Stropharia rugosoannulata*, are highly vulnerable to environmental contaminants, including antibiotics. This study addresses the question of whether antibiotics impact the food safety of *S. rugosoannulata*. The influence of antibiotics on *S. rugosoannulata* and the molecular mechanisms underlying this process were investigated. Based on our findings, we can confirm that, under the current level of antibiotic contamination, the growth of *S. rugosoannulata* remains unaffected by antibiotics, thus ensuring its safety.

CRediT authorship contribution statement

Wei Wan: Methodology. **Xingdong Yao:** Methodology. **Xiaohang Li:** Methodology. **Shuxue Zhao:** Writing – original draft, Software, Methodology, Formal analysis. **Chunhui Hu:** Writing – original draft, Software, Formal analysis, Data curation. **Jie Bai:** Conceptualization. **Lizhong Guo:** Supervision, Resources, Project administration, Funding acquisition. **Lili Xu:** Formal analysis. **Hao Yu:** Writing – review & editing, Supervision, Investigation, Funding acquisition, Formal analysis, Data curation, Conceptualization.

Declaration of Generative AI and AI-assisted technologies in the writing process

The authors declare that they did not use generative AI and AI-assisted technologies in the writing process.

Declaration of Competing Interest

The authors declare that they have no known competing financial interests or personal relationships that could have appeared to influence the work reported in this paper.

Data availability

Data will be made available on request.

Acknowledgements

This study was funded by Key R&D Program of Shandong Province (2021ZDSYS28), Shandong Edible Fungus Agricultural Technology System (SDAIT-07-02), and Qingdao Agricultural University Scientific Research Foundation (663-1119047, 660-2423332).

We wish to thank Central Laboratory of School of Life Science, Qingdao Agricultural University.

Appendix A. Supporting information

Supplementary data associated with this article can be found in the online version at doi:10.1016/j.jhazmat.2024.135099.

References

[1] Bombaywala, S., Mandpe, A., Paliya, S., Kumar, S., 2021. Antibiotic resistance in the environment: a critical insight on its occurrence, fate, and eco-toxicity. Environ Sci Pollut R 28 (20), 24889–24916. https://doi.org/10.1007/s11356-021-13143-x.
[2] Larsson, D.G.J., Flach, C.F., 2022. Antibiotic resistance in the environment. Nat Rev Microbiol 20, 257–269. https://doi.org/10.1038/s41579-021-00649-x.
[3] Chen, Q., Cui, H., Su, J., Penuelas, J., Zhu, Y., 2019. Antibiotic resistomes in plant microbiomes. Trends Plant Sci 24 (6), 530–541. https://doi.org/10.1016/j.tplants.2019.02.010.
[4] Geng, J., Liu, X., Wang, J., Li, S., 2022. Accumulation and risk assessment of antibiotics in edible plants grown in contaminated farmlands: a review. Sci Total Environ 853, 158616. https://doi.org/10.1016/j.scitotenv.2022.158616.
[5] Ben, Y., Fu, C., Hu, M., Liu, L., Wong, M., Zheng, C., 2019. Human health risk assessment of antibiotic resistance associated with antibiotic residues in the environment: a review. Environ Re 169, 483–493. https://doi.org/10.1016/j.envres.2018.11.040.
[6] Zeng, Q., Sun, J., Zhu, L., 2019. Occurrence and distribution of antibiotics and resistance genes in greenhouse and open-field agricultural soils in China. Chemosphere 224, 900–909. https://doi.org/10.1016/j.chemosphere.2019.02.167.
[7] Yin, Y., Zhu, D., Yang, G., Su, J., Duan, G., 2022. Diverse antibiotic resistance genes and potential pathogens inhabit in the phyllosphere of fresh vegetables. Sci Total Environ 815, 152851. https://doi.org/10.1016/j.scitotenv.2021.152851.
[8] Chen, J., Ying, G., Deng, W., 2019. Antibiotic residues in food: extraction, analysis, and human health concerns. J Agr Food Chem 67 (27), 7569–7586. https://doi.org/10.1021/acs.jafc.9b01334.
[9] Lu, H., Lou, H., Hu, J., Liu, Z., Chen, Q., 2020. Macrofungi: a review of cultivation strategies, bioactivity, and application of mushrooms. Compr Rev Food Sci F 19 (5), 2333–2356. https://doi.org/10.1111/1541-4337.12602.
[10] Bell, V., Silva, C.R.P.G., Guina, J., Fernandes, T.H., 2022. Mushrooms as future generation healthy foods. Front Nutr 9, 1050099. https://doi.org/10.3389/fnut.2022.1050099.
[11] Li, C., Xu, S., 2022. Edible mushroom industry in China: current state and perspectives. Appl Microbiol Biot 106 (11), 3949–3955. https://doi.org/10.1007/s00253-022-11985-0.
[12] Kapahi, M., 2018. Recent advances in cultivation of edible mushrooms. Biol Macrofungi 275–286. https://doi.org/10.1007/978-3-030-02622-6_13.
[13] Sánchez, C., 2010. Cultivation of Pleurotus ostreatus and other edible mushrooms. Appl Microbiol Biot 85 (5), 1321–1337. https://doi.org/10.1007/s00253-009-2343-7.
[14] Jurak, E., Kabel, M.A., Gruppen, H., 2014. Carbohydrate composition of compost during composting and mycelium growth of *Agaricus bisporus*. Carbohydr Polym 101, 281–288. https://doi.org/10.1016/j.carbpol.2013.09.050.
[15] Gaballah, M.S., Guo, J., Sun, H., Aboagye, D., Sobhi, M., Muhmood, A., et al., 2021. A review targeting veterinary antibiotics removal from livestock manure management systems and future outlook. Bioresour Technol 333, 125069. https://doi.org/10.1016/j.biortech.2021.125069.
[16] Marutescu, L.G., Jaga, M., Postolache, C., Barbuceanu, F., Milita, N.M., Romascu, L.M., et al., 2022. Insights into the impact of manure on the environmental antibiotic residues and resistance pool. Front Microbiol 13, 965132. https://doi.org/10.3389/fmicb.2022.965132.
[17] Zhang, L., Li, L., Sha, G., Liu, C., Wang, Z., Wang, L., 2020. Aerobic composting as an effective cow manure management strategy for reducing the dissemination of antibiotic resistance genes: an integrated meta-omics study. J Hazard Mater 386, 121895. https://doi.org/10.1016/j.jhazmat.2019.121895.
[18] Gu, J., Chen, C., Huang, X., Mo, J., Xie, Q., Zeng, Q., 2021. Occurrence and risk assessment of tetracycline antibiotics in soils and vegetables from vegetable fields in Pearl River Delta, South China. Sci Total Environ 776, 145959. https://doi.org/10.1016/j.scitotenv.2021.145959.
[19] Zhuo, R., Fan, F., 2021. A comprehensive insight into the application of white rot fungi and their lignocellulolytic enzymes in the removal of organic pollutants. Sci Total Environ 778, 146132. https://doi.org/10.1016/j.scitotenv.2021.146132.
[20] Delius, J., Emmerich, M., Özyurt, V., Hamscher, G., 2022. Biotransformation of tetracyclines by fungi: challenges and future research perspectives. J Agr Food Chem 70 (5), 1454–1460. https://doi.org/10.1021/acs.jafc.1c05121.
[21] Abadulla, E., Tzanov, T., Costa, S., Robra, K.H., Cavaco-Paulo, A., Gübitz, G.M., 2000. Decolorization and detoxification of textile dyes with a laccase from *Trametes hirsuta*. Appl Environ Micro 66 (8), 3357–3362. https://doi.org/10.1128/AEM.66.8.3357-3362.2000.
[22] Ding, H., Wu, Y., Zou, B., Lou, Q., Zhang, W., Zhong, J., et al., 2016. Simultaneous removal and degradation characteristics of sulfonamide, tetracycline, and quinolone antibiotics by laccase-mediated oxidation coupled with soil adsorption. J Hazard Mater 307, 350–358. https://doi.org/10.1016/j.jhazmat.2015.12.062.
[23] Torres-Duarte, C., Roman, R., Tinoco, R., Vazquez-Duhalt, R., 2009. Halogenated pesticide transformation by a laccase-mediator system. Chemosphere 77 (5), 687–692. https://doi.org/10.1016/j.chemosphere.2009.07.039.
[24] Suda, T., Hata, T., Kawai, S., Okamura, H., Nishida, T., 2012. Treatment of tetracycline antibiotics by laccase in the presence of 1-hydroxybenzotriazole.

Bioresour Technol 103 (1), 498–501. https://doi.org/10.1016/j.biortech.2011.10.041.
[25] Zou, M., Tian, W., Chu, M., Lu, Z., Liu, B., Xu, D., 2023. Magnetically separable laccase-biochar composite enable highly efficient adsorption-degradation of quinolone antibiotics: immobilization, removal performance and mechanisms. Sci Total Environ 879, 163057. https://doi.org/10.1016/j.scitotenv.2023.163057.
[26] Tang, S., Fan, T., Jin, L., Lei, P., Shao, C., Wu, S., et al., 2022. Soil microbial diversity and functional capacity associated with the production of edible mushroom *Stropharia rugosoannulata* in croplands. Peerj 10, e14130. https://doi.org/10.7717/peerj.14130.
[27] Scheibner, K., Hofrichter, M., Herre, A., Michels, J., Fritsche, W., 1997. Screening for fungi intensively mineralizing 2,4,6-trinitrotoluene. Appl Microbiol Biot 47 (4), 452–457. https://doi.org/10.1007/s002530050955.
[28] Kabiersch, G., Rajasärkkä, J., Ullrich, R., Tuomela, M., Hofrichter, M., Virta, M., et al., 2011. Fate of bisphenol A during treatment with the litter-decomposing fungi *Stropharia rugosoannulata* and *Stropharia coronilla*. Chemosphere 83 (3), 226–232. https://doi.org/10.1016/j.chemosphere.2010.12.094.
[29] Anasonye, F., Winquist, E., Kluczek-Turpeinen, B., Räsänen, M., Salonen, K., Steffen, K.T., et al., 2014. Fungal enzyme production and biodegradation of polychlorinated dibenzo-p-dioxins and dibenzofurans in contaminated sawmill soil. Chemosphere 110, 85–90. https://doi.org/10.1016/j.chemosphere.2014.03.079.
[30] Sen, K., Llewellyn, M., Taheri, B., Turner, R.J., Berglund, T., Maloney, K., 2023. Mechanism of fungal remediation of wetland water: *Stropharia rugosoannulata* as promising fungal species for the development of biofilters to remove clinically important pathogenic and antibiotic resistant bacteria in contaminated water. Front Microbiol 14, 1234586. https://doi.org/10.3389/fmicb.2023.1234586.
[31] Li, S., Zhao, S., Hu, C., Mao, C., Guo, L., Yu, Hailong, et al., 2022. Whole genome sequence of an edible mushroom *Stropharia rugosoannulata* (Daqiugaigu). J Fungi 8, 99. https://doi.org/10.3390/jof8020099.
[32] Han, Z., Wang, H., Zheng, J., Wang, S., Yu, S., Lu, L., 2023. Ultrafast synthesis of laccase-copper phosphate hybrid nanoflowers for efficient degradation of tetracycline antibiotics. Environ Res 216, 114690. https://doi.org/10.1016/j.envres.2022.114690.
[33] Zhang, Y., Zhou, J., Xu, Q., Cheng, J., Luo, Y., Yuan, Y., 2016. Exogenous cofactors for the improvement of bioremoval and biotransformation of sulfamethoxazole by *Alcaligenes faecalis*. Sci Total Environ 565, 547–556. https://doi.org/10.1016/j.scitotenv.2016.05.063.
[34] Xu, S., Chen, X., Wang, X., Sun, H., Hou, Z., Cheng, J., et al., 2022. Artificial microbial consortium producing oxidases enhanced the biotransformation efficiencies of multi-antibiotics. J Hazard Mater 439, 129674. https://doi.org/10.1016/j.jhazmat.2022.129674.
[35] Isaacson, T., Damasceno, C.M., Saravanan, R.S., He, Y., Catalá, C., Saladié, M., Rose, J.K., 2006. Sample extraction techniques for enhanced proteomic analysis of plant tissues. Nat Proto 1, 769–774. https://doi.org/10.1038/nprot.2006.102.
[36] Yu, H., Jiang, N., Yan, M., Cheng, X., Zhang, L., Zhai, D., et al., 2023. Comparative analysis of proteomes and transcriptomes revealed the molecular mechanism of development and nutrition of *Pleurotus giganteus* at different fruiting body development stages. Front Nutr 10, 1197983. https://doi.org/10.3389/fnut.2023.1197983.
[37] Tyanova, S., Temu, T., Sinitcyn, P., Carlson, A., Hein, M.Y., Geiger, T., et al., 2016. The Perseus computational platform for comprehensive analysis of (prote)omics data. Nat Methods 13, 731–740. https://doi.org/10.1038/nmeth.3901.
[38] Yu, H., Zhao, S., Guo, L., 2018. Novel Gene Encoding 5-Aminosalicylate 1,2-Dioxygenase from *Comamonas* sp. Strain QT12 and Catalytic Properties of the Purified Enzyme. J Bacteriol 200, e00395–17. https://doi.org/10.1128/JB.00395-17.
[39] Biasini, M., Bienert, S., Waterhouse, A., Arnold, K., Studer, G., Schmidt, T., et al., 2014. SWISS-MODEL: modelling protein tertiary and quaternary structure using evolutionary information. Nucleic Acids Res 42, W252–W258. https://doi.org/10.1093/nar/gku340.
[40] Yuan, S., Liu, Z., Yin, H., Dang, Z., Wu, P., Zhu, N., et al., 2019. Trace determination of sulfonamide antibiotics and their acetylated metabolites via SPE-LC-MS/MS in wastewater and insights from their occurrence in a municipal wastewater treatment plant. Sci Total Environ 653, 815–821. https://doi.org/10.1016/j.scitotenv.2018.10.417.
[41] Sushko, I., Novotarskyi, S., Körner, R., Pandey, A.K., Cherkasov, A., Li, J., et al., 2010. Applicability domains for classification problems: Benchmarking of distance to models for Ames mutagenicity set. J Chem Inf Model 50, 2094–2111. https://doi.org/10.1021/ci100253r.
[42] Caianelo, M., Rodrigues-Silva, C., Maniero, M.G., Diniz, V., Spina, M., Guimarães, J.R., 2021. Evaluation of residual antimicrobial activity and acute toxicity during the degradation of gatifloxacin by ozonation. Water Sci Technol 84, 225–236. https://doi.org/10.2166/wst.2021.208.
[43] Song, S., Han, M., Wang, X., Wang, S., Qin, W., Zhang, Y., et al., 2023. Fate of antibiotic resistance genes in cultivation substrate and its association with bacterial communities throughout commercial production of *Agaricus bisporus*. Ecotox Environ Safe 249, 114360. https://doi.org/10.1016/j.ecoenv.2022.114360.
[44] Lyu, J., Yang, L., Zhang, L., Ye, B., Wang, L., 2020. Antibiotics in soil and water in China-a systematic review and source analysis. Environ Pollut (Barking, Essex: 1987) 266, 115147. https://doi.org/10.1016/j.envpol.2020.115147.
[45] Yang, Y., Wei, F., Zhuo, R., Fan, F., Liu, H., Zhang, C., et al., 2013. Enhancing the laccase production and laccase gene expression in the white-rot fungus *Trametes velutina* 5930 with great potential for biotechnological applications by different metal ions and aromatic compounds. PloS One 8, e79307. https://doi.org/10.1371/journal.pone.0079307.
[46] Elisashvili, V., Kachlishvili, E., Khardziani, T., Agathos, S.N., 2010. Effect of aromatic compounds on the production of laccase and manganese peroxidase by white-rot basidiomycetes. J Ind Microbiol Biot 37, 1091–1096. https://doi.org/10.1007/s10295-010-0757-y.
[47] Zhang, H., Zhang, S., He, F., Qin, X., Zhang, X., Yang, Y., 2016. Characterization of a manganese peroxidase from white-rot fungus *Trametes* sp. 48424 with strong ability of degrading different types of dyes and polycyclic aromatic hydrocarbons. J Hazard Mater 320, 265–277. https://doi.org/10.1016/j.jhazmat.2016.07.065.
[48] Korcan, S.E., Ciğerci, İ.H., Konuk, M., 2012. White-rot fungi in bioremediation. Fungi Bioremediators 371–390. https://doi.org/10.1007/978-3-642-33811-3_16.
[49] Letten, A.D., Hall, A.R., Levine, J.M., 2021. Using ecological coexistence theory to understand antibiotic resistance and microbial competition. Nat Ecol Evol 5, 431–441. https://doi.org/10.1038/s41559-020-01385-w.
[50] Barr, D.P., Aust, S.D., 1994. Pollutant degradation by white rot fungi. Rev Environ Contam T 138 49–72. https://doi.org/10.1007/978-1-4612-2672-7_3.
[51] Zhang, H., Liu, X., Liu, B., Sun, F., Jing, L., Shao, L., et al., 2023. Synergistic degradation of Azure B and sulfanilamide antibiotics by the white-rot fungus *Trametes versicolor* with an activated ligninolytic enzyme system. J Hazard Mater 458, 131939. https://doi.org/10.1016/j.jhazmat.2023.131939.
[52] Yang, J., Lin, Y., Yang, X., Ng, T.B., Ye, X., Lin, J., 2017. Degradation of tetracycline by immobilized laccase and the proposed transformation pathway. J Hazard Mater 322, 525–531. https://doi.org/10.1016/j.jhazmat.2016.10.019.
[53] Weng, S., Liu, S., Lai, H., 2013. Application parameters of laccase-mediator systems for treatment of sulfonamide antibiotics. Bioresour Technol 141, 152–159. https://doi.org/10.1016/j.biortech.2013.02.093.
[54] Sellami, K., Couvert, A., Nasrallah, N., Maachi, R., Abouseoud, M., Amrane, A., 2022. Peroxidase enzymes as green catalysts for bioremediation and biotechnological applications: a review. Sci Total Environ 806, 150500. https://doi.org/10.1016/j.scitotenv.2021.150500.
[55] Yang, L., Qiao, B., Xu, Q., Liu, S., Yuan, Y., Cheng, J., 2021. Biodegradation of sulfonamide antibiotics through the heterologous expression of laccases from bacteria and investigation of their potential degradation pathways. J Hazard Mater 416, 125815. https://doi.org/10.1016/j.jhazmat.2021.125815.
[56] Liu, C., Zhang, W., Qu, M., Pan, K., Zhao, X., 2020. Heterologous Expression of Laccase From *Lentinula edodes* in *Pichia pastoris* and Its Application in Degrading Rape Straw. Front Microbiol 11, 1086. https://doi.org/10.3389/fmicb.2020.01086.
[57] Ramírez-Cavazos, L.I., Junghanns, C., Ornelas-Soto, N., Cárdenas-Chávez, D.L., Hernández-Luna, C., Demarche, P., et al., 2014. Purification and characterization of two thermostable laccases from *Pycnoporus sanguineus* and potential role in degradation of endocrine disrupting chemicals. J Mol Catal B-Enzym 108, 32–42. https://doi.org/10.1016/j.molcatb.2014.06.006.
[58] Luo, Q., Chen, Y., Xia, J., Wang, K., Cai, Y., Liao, X., et al., 2018. Functional expression enhancement of *Bacillus pumilus* CotA-laccase mutant WLF through site-directed mutagenesis. Enzym Micro Tech 109, 11–19. https://doi.org/10.1016/j.enzmictec.2017.07.013.
[59] Shao, B., Liu, Z., Zeng, G., Liu, Y., Yang, X., Zhou, C., et al., 2019. Immobilization of laccase on hollow mesoporous carbon nanospheres: Noteworthy immobilization, excellent stability and efficacious for antibiotic contaminants removal. J Hazard Mater 362, 318–326. https://doi.org/10.1016/j.jhazmat.2018.08.069.
[60] Margot, J., Copin, P., von Gunten, U., Barry, D.A., Holliger, C., 2015. Sulfamethoxazole and isoproturon degradation and detoxification by a laccase-mediator system: Influence of treatment conditions and mechanistic aspects. Biochem Eng J 103, 47–59. https://doi.org/10.1016/j.bej.2015.06.008.
[61] Potthast, A., Rosenau, T., Fischer, K., 2001. Oxidation of benzyl alcohols by the laccase-mediator system (LMS) a comprehensive kinetic description. Holzforschung 55, 47–56. https://doi.org/10.1515/HF.2001.008.
[62] Johannes, C., Majcherczyk, A., 2000. Natural mediators in the oxidation of polycyclic aromatic hydrocarbons by laccase mediator systems. Appl Environ Micro 66, 524–528. https://doi.org/10.1128/AEM.66.2.524-528.2000.
[63] Ibrahim, V., Volkova, N., Pyo, S.H., Mamo, G., Hatti-Kaul, R., 2013. Laccase catalysed modification of lignin subunits and coupling to *p*-aminobenzoic acid. J Mol Catal B-Enzym 97, 45–53. https://doi.org/10.1016/j.molcatb.2013.07.014.
[64] Ouyang, B., Xu, W., Zhang, W., Guang, C., Mu, W., 2022. Efficient removal of sulfonamides and tetracyclines residues by the laccase-mediator system employing a novel laccase from *Lysinibacillus fusiformis*. J Environ Chem Eng 10, 108809. https://doi.org/10.1016/j.jece.2022.108809.
[65] Tian, Q., Dou, X., Huang, L., Wang, L., Meng, D., Zhai, L., et al., 2020. Characterization of a robust cold-adapted and thermostable laccase from *Pycnoporus* sp. SYBC-L10 with a strong ability for the degradation of tetracycline and oxytetracycline by laccase-mediated oxidation. J Hazard Mater 382, 121084. https://doi.org/10.1016/j.jhazmat.2019.121084.
[66] Riva, S., 2006. Laccases: blue enzymes for green chemistry. Trends Biotechnol 24, 219–226. https://doi.org/10.1016/j.tibtech.2006.03.006.
[67] Kumar, S.V.S., Phale, P.S., Durani, S., Wangikar, P.P., 2003. Combined sequence and structure analysis of the fungal laccase family. Biotechnol Bioeng 83, 386–394. https://doi.org/10.1002/bit.10681.
[68] Wei, R., He, T., Zhang, S., Zhu, L., Shang, B., Li, Z., et al., 2019. Occurrence of seventeen veterinary antibiotics and resistant bacterias in manure-fertilized vegetable farm soil in four provinces of China. Chemosphere 215, 234–240. https://doi.org/10.1016/j.chemosphere.2018.09.152.
[69] Bueno, I., He, H., Kinsley, A.C., Ziemann, S.J., Degn, L.R., Nault, A.J., et al., 2023. Biodegradation, photolysis, and sorption of antibiotics in aquatic environments: a scoping review. Sci Total Environ 897, 165301. https://doi.org/10.1016/j.scitotenv.2023.165301.

[70] Li, Y., Wu, X., Mo, C., Tai, Y., Huang, X., Xiang, L., 2011. Investigation of sulfonamide, tetracycline, and quinolone antibiotics in vegetable farmland soil in the Pearl River Delta area, southern China. J Agr Food Chem 59, 7268–7276. https://doi.org/10.1021/jf1047578.

[71] Shi, L., Ma, F., Han, Y., Zhang, X., Yu, H., 2014. Removal of sulfonamide antibiotics by oriented immobilized laccase on Fe_3O_4 nanoparticles with natural mediators. J Hazard Mater 279, 203–211. https://doi.org/10.1016/j.jhazmat.2014.06.070.

[72] Li, R., Zhou, T., Khan, A., Ling, Z., Sharma, M., Feng, P., et al., 2021. Feed-additive of bioengineering strain with surface-displayed laccase degrades sulfadiazine in broiler manure and maintains intestinal flora structure. J Hazard Mater 406, 124440. https://doi.org/10.1016/j.jhazmat.2020.124440.

[73] Blánquez, A., Guillén, F., Rodríguez, J., Arias, M.E., Hernández, M., 2016. The degradation of two fluoroquinolone based antimicrobials by SilA, an alkaline laccase from *Streptomyces ipomoeae*. World J Micro Biot 32, 52. https://doi.org/10.1007/s11274-016-2032-5.

[74] Vojdanitalab, K., Jafari-Nodoushan, H., Mojtabavi, S., Shokri, M., Jahandar, H., Faramarzi, M.A., 2022. Instantaneous synthesis and full characterization of organic-inorganic laccase-cobalt phosphate hybrid nanoflowers. Sci Rep-Uk 12, 9297. https://doi.org/10.1038/s41598-022-13490-w.

[75] Ashrafi, S.D., Nasseri, S., Alimohammadi, M., Mahvi, A.H., Faramarzi, M.A., 2020. Application of free and immobilized laccase for removal and detoxification of fluoroquinolones from aqueous solution. Glob Nest J 22, 240–249. https://doi.org/10.30955/gnj.002973.

[76] Boerjan, W., Ralph, J., Baucher, M., 2003. Lignin biosynthesis. Annu Rev Plant Biol 54, 519–546. https://doi.org/10.1146/annurev.arplant.54.031902.134938.

[77] Tang, Y., Li, W., Muhammad, Y., Jiang, S., Huang, M., Zhang, H., et al., 2021. Fabrication of hollow covalent-organic framework microspheres via emulsion-interfacial strategy to enhance laccase immobilization for tetracycline degradation. Chem Eng J 421, 129743. https://doi.org/10.1016/j.cej.2021.129743.

[78] Sun, K., Huang, Q., Li, S., 2017. Transformation and toxicity evaluation of tetracycline in humic acid solution by laccase coupled with 1-hydroxybenzotriazole. J Hazard Mater 331, 182–188. https://doi.org/10.1016/j.jhazmat.2017.02.058.

[79] Wen, X., Shen, C., Niu, C., Lai, D., Zhu, M., Sun, J., et al., 2019. Attachment of Ag/AgCl nanoparticles on $CdMoO_4$ microspheres for effective degradation of doxycycline under visible light irradiation: degradation pathways and mineralization activity. J Mol Liq 288, 111063. https://doi.org/10.1016/j.molliq.2019.111063.

[80] Zhang, J., Zhao, Y., Yang, M., Jiang, H., Wang, B., Jia, Y., et al., 2022. Efficient electrocatalytic degradation of doxycycline hydrochloride in wastewater by Ni/MWCNTs-OH on modified Ti. J Water Process Eng 50, 103187. https://doi.org/10.1016/j.jwpe.2022.103187.

[81] Chen, Y., Sun, X., Huang, Y., Guo, D., Zheng, L., Liu, Y., et al., 2022. Hierarchical $Bi_{0.5}Fe_{0.5}VO_4$/honeycomb ceramic plate synergize plasma induce multi-catalysis by constructing a plasma-catalyst system for organic pollutant degradation. Sep Purif Technol 286, 120444. https://doi.org/10.1016/j.seppur.2022.120444.

[82] Yang, S., Che, D., 2017. Degradation of aquatic sulfadiazine by Fe^0/persulfate: kinetics, mechanisms, and degradation pathway. Rsc Adv 7, 42233–42241. https://doi.org/10.1039/C7RA07920F.

[83] Feng, Y., Wu, D., Liao, C., Deng, Y., Zhang, T., Shih, K., 2016. Red mud powders as low-cost and efficient catalysts for persulfate activation: Pathways and reusability of mineralizing sulfadiazine. Sep Purif Technol 167, 136–145. https://doi.org/10.1016/j.seppur.2016.04.051.

[84] Yadav, M.S.P., Neghi, N., Kumar, M., Varghese, G.K., 2018. Photocatalytic-oxidation and photo-persulfate-oxidation of sulfadiazine in a laboratory-scale reactor: Analysis of catalyst support, oxidant dosage, removal-rate and degradation pathway. J Environ Manag 222, 164–173. https://doi.org/10.1016/j.jenvman.2018.05.052.

[85] Chao, C., Zhao, Y., Guan, H., Liu, G., Hu, Z., Zhang, B., 2017. Improved performance of immobilized laccase on poly(diallyldimethylammonium chloride) functionalized halloysite for 2,4-dichlorophenol degradation. Environ Eng Sci 34, 762–770. https://doi.org/10.1089/ees.2016.0549.

[86] Chen, L., Ji, H., Qi, J., Huang, T., Wang, C., Liu, W., 2021. Degradation of acetaminophen by activated peroxymonosulfate using $Co(OH)_2$ hollow microsphere supported titanate nanotubes: Insights into sulfate radical production pathway through $CoOH^+$ activation. Chem Eng J 406, 126877. https://doi.org/10.1016/j.cej.2020.126877.